6110 *Inorg. Chem.* **2010**, *49*, 6110–6123
DOI: 10.1021/ic100717w

Inorganic Chemistry
Article

Reduced *N*-Alkyl Substituted Bis(imino)pyridine Cobalt Complexes: Molecular and Electronic Structures for Compounds Varying by Three Oxidation States

Amanda C. Bowman,[†] Carsten Milsmann,[‡] Eckhard Bill,[‡] Emil Lobkovsky,[†] Thomas Weyhermüller,[†] Karl Wieghardt,*[,‡] and Paul J. Chirik*[,†]

[†]*Department of Chemistry and Chemical Biology, Baker Laboratory, Cornell University, Ithaca, New York 14853, and* [‡]*Max-Planck Institute for Bioinorganic Chemistry, Stiftstrasse 34-36, D-45470 Mülheim an der Ruhr, Germany*

Received April 14, 2010

The stepwise 1−3 electron reduction of the *N*-alkyl substituted bis(imino)pyridine cobalt dichloride complexes, (^{R}APDI)$CoCl_2$, was studied where ^{R}APDI = 2,6-(RN═CMe)$_2C_5H_3N$, R = C_6H_{11} (Cy), $CHMe_2$ (^{i}Pr). One electron reduction with either zinc metal or $NaBEt_3H$ furnished the bis(imino)pyridine cobalt monochloride compounds, (^{R}APDI)CoCl. X-ray diffraction on the (^{iPr}APDI)CoCl derivative established a distortion from square planar geometry where the chloride ligand is lifted out of the idealized cobalt-chelate plane. Superconducting Quantum Interference Device (SQUID) magnetometry on both compounds established spin crossover behavior with an $S = 1$ state being predominant at room temperature. Computational studies, in combination with experimental results, establish that the triplet spin isomer arises from a high spin Co(II) center ($S_{Co} = 3/2$) antiferromagnetically coupled to a bis(imino)pyridine chelate radical anion, $[PDI]^{-}$ ($S_{PDI} = 1/2$). At lower temperatures, the Co(II) ion undergoes a spin transition to the low spin form ($S_{Co} = 1/2$) and antiferromagnetic coupling gives rise to the observed diamagnetic ground state. Replacing the chloride ligand with a methyl group, namely (^{R}APDI)$CoCH_3$, also yielded distorted compounds, albeit less pronounced, that are diamagnetic at room temperature. Two electron reduction of the (^{R}APDI)$CoCl_2$ derivatives with excess 0.5% sodium amalgam or 2 equiv of $NaBEt_3H$ furnished the bis(chelate)cobalt complexes, (^{R}APDI)$_2$Co, while three electron reduction with 3 equiv of sodium naphthalenide yielded the cobalt dinitrogen anions, $[Na(solv)_3][(^{R}APDI)CoN_2]$ (solv = THF, Et_2O). Both bis(chelate) compounds were crystallographically characterized and determined to have $S = 3/2$ ground states by SQUID magnetometry and electron paramagnetic resonance (EPR) spectroscopy. Computational studies, in combination with metrical parameters determined from X-ray diffraction, establish a high spin ($S_{Co} = 3/2$) cobalt(II) center with two bis(imino)pyridine chelate radical anions. Antiferromagnetic coupling between the two chelate centered radicals is mediated by a doubly occupied t_{2g} cobalt orbital and gives rise to the observed overall quartet ground state.

Introduction

Bis(imino)pyridine ligands, 2,6-(R^1N═CR^2)$_2C_5H_3N$ (R^1 = alkyl, aryl, amino; R^2 = H, Me), have a long-standing history in the classical Werner-type coordination chemistry of cobalt. Because of the early successes of terpyridine ligands, attention was devoted to preparing easily accessed and modular analogues that preserved the tridendate, meridional "N_3" coordination motif.[1] The first examples of bis(imino)pyridine cobalt compounds were six-coordinate, dicationic bis(chelate) derivatives of cobalt(II), for example, $[(PDI)_2Co]X_2$ (X = Cl, I, ClO_4). These molecules proved to be early experimental examples of the success of ligand field theory as the values of Δ_{Oct} and pairing energies were measured for both the low and the high spin forms of the d^7 ion.[2,3] Magnetic data on these bis(chelate) cobalt dications also proved interesting. Depending on the specific imine substituents and counterions, magnetic susceptibilities consistent with the spin only values expected for the $^4T_1$ and ^2E extremes were observed as well as examples with "anomalous magnetic behavior" where temperature dependent μ_{eff} values between the pure high and low spin limits were measured.[3,4] Initially, a simple two-state model was proposed where an equilibrium between low and high spin forms was used to account for the observed magnetic susceptibilities.[3] More detailed studies later showed that such an explanation was likely oversimplified as mixing of the $^4T_1$ and ^2E states near the crossing point produces a variety of thermally accessible states where a Boltzman distribution would account for the observed magnetic moments.[4] In addition to magnetic studies, the hexacoordinate bis(chelate) cobalt(II)

*To whom correspondence should be addressed. E-mail: pc92@cornell.edu (P.J.C.).

(1) Lions, F.; Martin, K. V. *J. Am. Chem. Soc.* **1957**, *79*, 2733.
(2) Figgins, P. E.; Busch, D. H. *J. Am. Chem. Soc.* **1960**, *82*, 820.
(3) Stouffer, R. C.; Hadley, W. B.; Busch, D. H. *J. Am. Chem. Soc.* **1961**, *83*, 3732.
(4) Stouffer, R. C.; Smith, D. W.; Clevenger, E. A.; Norris, T. E. *Inorg. Chem.* **1966**, *5*, 1167.

 Published on Web 06/11/2010

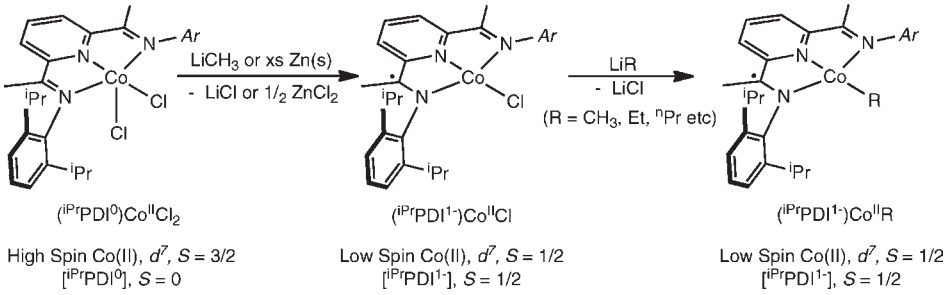

Figure 1. Synthesis and electronic structures of aryl-substituted bis(imino)pyridine cobalt chloride and alkyl compounds.

dications were some of the first examples of Co(II) coordination compounds to be studied by both solid state and solution electron paramagnetic resonance (EPR) spectroscopy.[5]

Following these seminal studies, manipulation of the ligand architecture was explored and new coordination numbers and structural types of the resulting cobalt compounds were obtained. Introduction of larger *N*-imine substituents or replacing the in-plane backbone hydrogens with methyl groups resulted in more sterically protected ligands that allowed isolation of so-called "1:1" bis(imino)pyridine cobalt(II) compounds.[6−8] In each case examined, high spin Co(II), d^7 centers ($S_{Co} = 3/2$) were observed. Brookhart and Gibson's independent use of bis(imino)pyridines with sterically demanding *N*-aryl substituents, ^{Ar}PDI where ^{Ar}PDI = 2,6-(2,6-R_2-C_6H_3N=$CMe)_2C_5H_3N$, R = ^{i}Pr, Et, Me, H, etc., produced a class of cobalt(II) dihalide complexes that when activated with excess methylaluminoxane (MAO) were extremely active catalysts for olefin polymerization.[9−12] These landmark discoveries renewed interest in the fundamental coordination chemistry and electronic structure of bis(imino)pyridine cobalt compounds, particularly in the context of defining and understanding the propagating species.

Treatment of one of the prototypical olefin polymerization precatalysts, (^{iPr}PDI)$CoCl_2$ (^{iPr}PDI = 2,6-(2,6-$^i Pr_2$−C_6H_3N=$CMe)_2C_5H_3N$) with alkyl lithiums,[13] Grignard reagents,[14,15] or zinc metal[14] resulted in one electron reduction to yield the square planar, diamagnetic cobalt monochloride, (^{iPr}PDI)CoCl. Subsequent alkylation of this species furnished a family of the desired cobalt alkyls, (^{iPr}PDI)CoR (R = Me, Et, ^{n}Pr, ^{n}Bu) (Figure 1), as diamagnetic solids.[16−18] Analysis of these compounds by ^{1}H NMR spectroscopy and density functional theory (DFT) calculations established that these apparent Co(I) derivatives were actually composed of low-spin Co(II) ($S_{Co} = 1/2$) metal centers antiferromagnetically coupled to bis(imino)pyridine chelate radical anions ($S_{PDI} = 1/2$).[19] The computational studies also established low-lying, energetically accessible triplet excited states that were likely the origin of the anomalous upfield ^{1}H NMR chemical shifts observed for the in-plane imine methyl backbones.[19,20] These studies, along with the electrochemical work of Toma[21,22] and the preparative and spectroscopic experiments of Wieghardt and co-workers,[23,24] provided the foundation for establishing the redox-activity of the bis(imino)pyridine chelate[25−27] and likely the importance of this phenomenon in base metal catalysis.[28,29] Notably, the reduction of (^{iPr}PDI)$CoCl_2$ to (^{iPr}PDI)CoCl occurs at the ligand, preserving the Co(II) oxidation state, although a change from high spin to low spin accompanies chelate reduction because of the increased field strength of the chelate radical anion (Figure 1).

Given the rich chemistry associated with the bis(imino)pyridine iron dinitrogen complex, (^{iPr}PDI)$Fe(N_2)_2$,[30] our collaborative effort recently explored the synthesis and spectroscopy of related cobalt dinitrogen complexes. Reduction of the Brookhart−Gibson cobalt dihalide precursor, (^{iPr}PDI)$CoCl_2$, with excess 0.5% sodium amalgam under an N_2 atmosphere yielded the neutral, square planar cobalt dinitrogen compound, (^{iPr}PDI)CoN_2.[31] Performing the reduction of

(5) Schmidt, J. G.; Brey, W. S.; Stoufer, R. C. *Inorg. Chem.* **1967**, *6*, 268.
(6) Curry, J. D.; Robinson, M. A.; Busch, D. H. *Inorg. Chem.* **1967**, *6*, 1570.
(7) Sacconi, L.; Morassi, R.; Midollini, S. *J. Chem. Soc., A* **1968**, 1510.
(8) Davis, R. N.; Tanski, J. M.; Adrian, J. C.; Tyler, L. A. *Inorg. Chim. Acta* **2007**, *360*, 3061.
(9) Bianchini, C.; Giambastiani, G.; Rios, I. G.; Mantovani, G.; Meli, A.; Segarra, A. M. *Coord. Chem. Rev.* **2006**, *250*, 1391.
(10) Britovsek, G. J. P.; Gibson, V. C.; Kimberley, B. S.; Maddox, S. J.; Solan, G. A.; White, A. J. P.; Williams, D. J. *Chem. Commun.* **1998**, 849.
(11) (a) Small, B. M.; Brookhart, M. *J. Am. Chem. Soc.* **1998**, *120*, 7143. (b) Small, B. L.; Brookhart, M.; Bennett, A. M. A. *J. Am. Chem. Soc.* **1998**, *120*, 4049.
(12) Britovsek, G. J. P.; Bruce, M.; Gibson, V. C.; Kimberely, B. S.; Maddox, P. J.; Mastroianni, S.; McTavish, S. J.; Redshaw, C.; Solan, G. A.; Strömberg, S.; White, A. J. P.; Williams, D. J. *J. Am. Chem. Soc.* **1999**, *121*, 8728.
(13) Kooistra, T. M.; Knijnenburg, Q.; Smits, J. M. M.; Horton, A. D.; Budzelaar, P. H. M.; Gal, A. W. *Angew. Chem., Int. Ed.* **2001**, *40*, 4719.
(14) Gibson, V. C.; Humphries, M. J.; Tellmann, K. P.; Wass, D. F.; White, A. J. P.; Williams, D. J. *Chem. Commun.* **2001**, 2252.
(15) Steffen, W.; Blömker, T.; Kleigrewe, N.; Kehr, G.; Fröhlich, R.; Erker, G. *Chem. Commun.* **2004**, 1188.
(16) Gibson, V. C.; Tellmann, K. P.; Humphries, M. J.; Wass, D. F. *Chem. Commun.* **2002**, 2316.
(17) Tellmann, K. P.; Humphries, M. J.; Rzepa, H. S.; Gibson, V. C. *Organometallics* **2004**, *23*, 5503.
(18) Kleigrewe, N.; Steffen, W.; Blömker, T.; Kehr; Fröhlich, R.; Wibbeling, B.; Erker, G.; Wasilke, J.-C.; Wu, G.; Bazan, G. C. *J. Am. Chem. Soc.* **2005**, *127*, 13955.
(19) Knijnenburg, Q.; Hetterscheid, D.; Kooistra, T. M.; Budzelaar, P. H. M. *Eur. J. Inorg. Chem.* **2004**, 1204.
(20) Humphries, M. J.; Tellmann, K. P.; Gibson, V. C.; White, A. J. P.; Williams, D. J. *Organometallics* **2005**, *24*, 2039–2050.
(21) Kuwabara, I. H.; Comninos, F. C. M.; Pardini, V. L.; Viertler, H.; Toma, H. E. *Electrochim. Acta* **1994**, *39*, 2401.
(22) Toma, H. E.; Chavez-Gil, T. E. *Inorg. Chim. Acta* **1997**, *257*, 197.
(23) de Bruin, B.; Bill, E.; Bothe, E.; Weyermüller, T.; Wieghardt, K. *Inorg. Chem.* **2000**, *39*, 2936.
(24) Budzelaar, P. H. M.; de Bruin, B.; Gal, A. W.; Wieghardt, K.; van Lenthe, J. H. *Inorg. Chem.* **2001**, *40*, 4649.
(25) Chaudhuri, P.; Wieghardt, K. *Prog. Inorg. Chem.* **2001**, *50*, 151.
(26) (a) Knijnenburg, Q.; Gambarotta, S.; Budzelaar, P. H. M. *Dalton Trans.* **2006**, 5442. (b) Bart, S. C.; Chlopek, K.; Bill, E.; Bouwkamp, M. W.; Lobkovsky, E.; Neese, F.; Wieghardt, K.; Chirik, P. J. *J. Am. Chem. Soc.* **2006**, *128*, 13901.
(27) Butin, K. P.; Beloglazkina, E. K.; Zyk, N. V. *Russ. Chem. Rev.* **2005**, *74*, 531.
(28) Bouwkamp, M. W.; Bowman, A. C.; Lobkovsky, E.; Chirik, P. J. *J. Am. Chem. Soc.* **2006**, *128*, 13340.
(29) Sylvester, K. T.; Chirik, P. J. *J. Am. Chem. Soc.* **2009**, *131*, 8772.
(30) Bart, S. C.; Lobkovsky, E.; Chirik, P. J. *J. Am. Chem. Soc.* **2004**, *126*, 13794.
(31) Bowman, A. C.; Milsmann, C.; Atienza, C. C. H.; Lobkovsky, E.; Wieghardt, K.; Chirik, P. J. *J. Am. Chem. Soc.* **2010**, *132*, 1676.

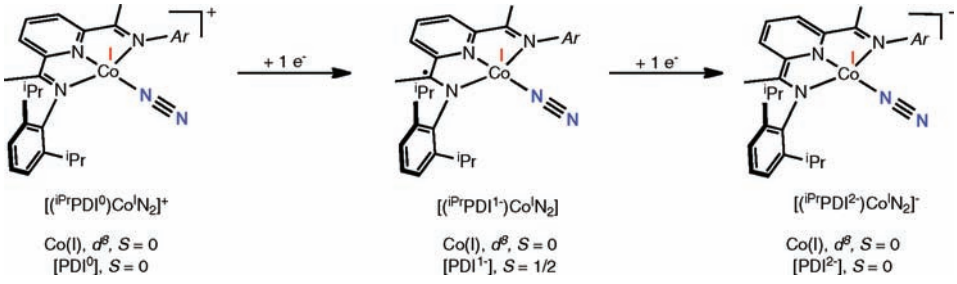

Figure 2. Electronic structure summary for bis(imino)pyridine cobalt dinitrogen complexes over three formal oxidation states.

(^{iPr}PDI)$CoCl_2$ with 3 equiv of sodium naphthalenide furnished the three-electron reduced cobalt dinitrogen anion, [(^{iPr}PDI)CoN_2]$^-$. These two compounds, in conjunction with the previously reported cobalt dinitrogen cation, [(^{iPr}PDI)CoN_2]$^+$,[32] allow evaluation of the electronic structure of the same core structure over three different formal oxidation states (Figure 2). Our combined synthetic, spectroscopic and computational studies established that the low-spin cobalt(I), d^8 electronic configuration is preserved throughout the series and that the redox-events are confined to the bis(imino)pyridine chelate. For example, in the cation, [(^{iPr}PDI)CoN_2]$^+$, the chelate is neutral while at the opposite extreme, the dinitrogen anion, [(^{iPr}PDI)CoN_2]$^-$, has the bis(imino)pyridine as a closed-shell dianion.

Because of the successes of bis(imino)pyridine ligands in supporting base metal polymerization catalysts,[9] the majority of recent studies on reduced versions of these compounds have focused on compounds with *N*-aryl substituted chelates. In iron chemistry, our laboratories recently explored the two electron reduction chemistry of the *N*-alkyl substituted bis(imino)pyridine iron dibromides, (^{R}APDI)$FeBr_2$ (^{R}APDI = 2,6-(RN=CMe)$_2C_5H_3N$; R = Cy, ^{i}Pr, *cis*-myrtanyl).[33] In each case, the neutral bis(chelate) iron complex, (^{R}APDI)$_2$Fe, was isolated. Magnetic measurements, metrical parameters from X-ray structures, Mössbauer spectroscopy, and open-shell, broken-symmetry DFT calculations established that the experimentally observed $S = 1$ ground states arise from antiferromagnetic coupling of the high spin ferrous ($S_{Fe} = 2$) centers with two bis(imino)pyridine radical anions ($S_{PDI} = 1/2$). In cobalt chemistry, Budzelaar and co-workers reported studies of the electronic structure of square planar bis(imino)pyridine cobalt halide, alkyl, and hydride compounds, (^{R1}APDI)$CoCH_2SiMe_3$ (R^1 = *n*-C_6H_{13}, *n*-$C_{18}H_{37}$), with *N*-alkyl substituted chelates.[19] No differences in electronic or molecular structure were noted between these compounds and the more well-studied *N*-arylated derivatives. Here we describe synthetic, spectroscopic and computational studies into the one, two, and three-electron reduction products of *N*-alkyl substituted bis(imino)pyridine cobalt dichlorides, (^{R}APDI)$CoCl_2$ (R = Cy, ^{i}Pr) and discover magnetic behavior, including spin crossover phenomena, structural distortions, and electronic structures distinct from the previously studied *N*-aryl substituted compounds.

Results and Discussion

Synthesis and Electronic Structure of *N*-Alkyl Bis(imino)pyridine Cobalt Chloride and Methyl Complexes. One electron reduction of the *N*-alkyl substituted bis(imino)pyridine cobalt dichloride complexes, (^{Cy}APDI)$CoCl_2$[8] and (^{iPr}APDI)$CoCl_2$, to form the corresponding cobalt monochloride compounds was initially explored. Stirring a toluene solution of either cobalt dichloride with 1 equiv of $NaBEt_3H$ in toluene followed by filtration and recrystallization from pentane yielded (^{Cy}APDI)CoCl and (^{iPr}APDI)CoCl as red-brown (63%) and mauve (60%) crystalline solids, respectively (eq 1). Both (^{Cy}APDI)CoCl and (^{iPr}APDI)CoCl were also prepared by stirring the corresponding cobalt dichloride complexes with excess zinc metal in toluene at 45 °C.

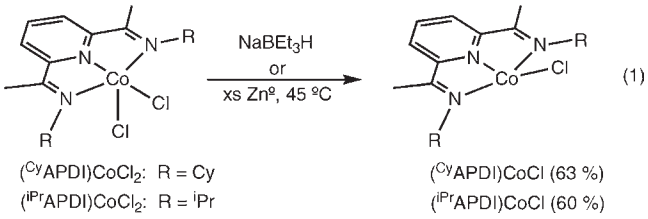

(1)

At this point, it is useful to comment on the representation of the structures in the equations, figures, and schemes. For the results of the synthetic work, the bis(imino)pyridine chelate will be drawn in its innocent, neutral form. Once the spectroscopic, magnetic, crystallographic, and computational studies are presented and the oxidation states of both the chelate and metal defined will the molecules be drawn with a more accurate depiction of the redox activity of the bis(imino)pyridine.

In contrast to the previously reported diamagnetic aryl-substituted bis(imino)pyridine chloride complexes,[14,15] both (^{Cy}APDI)CoCl and (^{iPr}APDI)CoCl are paramagnetic at 23 °C. Each compound exhibits the same number of paramagnetically broadened and shifted ^{1}H NMR resonances expected for C_{2v} symmetric molecules. The chemical shift dispersion for (^{Cy}APDI)CoCl is larger than that for (^{iPr}APDI)CoCl. As is typical for compounds of this type, the hydrogens on the chelate that are in the plane of the metal experience the largest deviations from their diamagnetic reference values. For (^{Cy}APDI)CoCl in benzene-d_6 at 23 °C, the imine methyl group was located at −22.8 ppm while the *meta* and *para*-pyridine hydrogens were identified at 12.1 and 66.3 ppm, respectively. For (^{iPr}APDI)CoCl, these same peaks were located at −12.6, 9.5, and 41.6 ppm.

The solid state structure of one example, (^{iPr}APDI)CoCl, was determined by X-ray diffraction at 173 K. A representation of the solid state structure is presented in Figure 3, and selected bond distances and angles are presented in Table 1. In contrast to rigorously square planar aryl-substituted bis(imino)pyridine cobalt chloride compounds such as (^{iPr}PDI)CoCl,[14] the overall

(32) Gibson, V. C.; Humphries, M. J.; Tellmann, K. P.; Wass, D. F.; White, A. J. P.; Williams, D. J. *Chem. Commun.* **2001**, 2252.
(33) Wile, B. M.; Trovitch, R. J.; Bart, S. C.; Tondreau, A. M.; Lobkovsky, E.; Milsmann, C.; Bill, E.; Wieghardt, K.; Chirik, P. J. *Inorg. Chem.* **2009**, *48*, 4190.

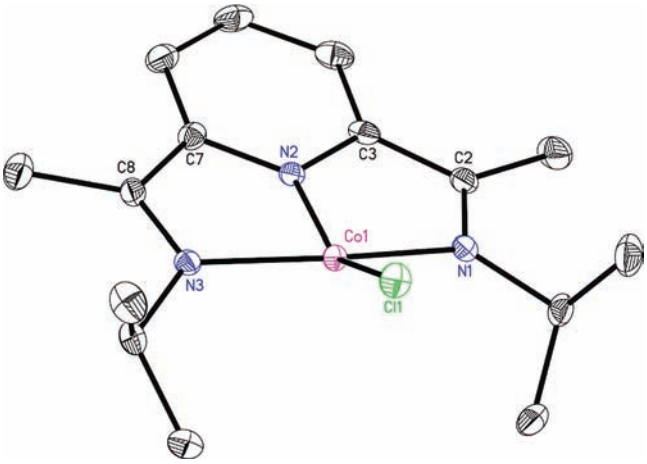

Figure 3. Molecular structure of (^{iPr}APDI)CoCl at 30% probability ellipsoids. Hydrogen atoms omitted for clarity.

Table 1. Selected Bond Distances (Å) and Angles (deg) for (^{iPr}APDI)CoCl, (^{iPr}PDI)CoCl,[14] (^{iPr}APDI)CoMe, and (^{iPr}PDI)CoMe.[14]

	(^{iPr}APDI)-CoCl	(^{iPr}PDI)-CoCl	(^{iPr}APDI)-CoMe	(^{iPr}PDI)-CoMe
Co−N_{imine}	1.9334(15)	1.916(3)	1.9103(16)	1.907(3)
	1.9203(16)	1.912(3)	1.9228(16)	1.903(3)
Co−$N_{pyridine}$	1.7870(16)	1.797(3)	1.8072(16)	1.834(3)
Co−X	2.2188(6)	2.1807(10)	1.967(2)	1.960(4)
N_{imine}−C_{imine}	1.314(3)	1.322(5)	1.326(2)	1.335(4)
	1.321(3)	1.317(5)	1.326(2)	1.329(4)
C_{imine}−C_{ipso}	1.435(3)	1.444(5)	1.440(3)	1.443(5)
	1.438(3)	1.435(5)	1.434(3)	1.434(6)
C_{ipso}−$N_{pyridine}$	1.371(2)	1.373(5)	1.373(2)	1.366(4)
	1.371(2)	1.369(6)	1.383(2)	1.365(4)

geometry of (^{iPr}APDI)CoCl is significantly distorted with an N_{pyr}−Co−Cl bond angle of 150.73(5)°. The isopropyl imine substituents are oriented essentially orthogonal to the cobalt-chelate plane with the methine hydrogens directed toward the in-plane backbone methyl groups. The Co−Cl bond length of 2.2188(6) Å is slightly elongated from the value of 2.1807(10) Å found in (^{iPr}PDI)CoCl.[14] The metrical parameters for the bis(imino)pyridine chelate are diagnostic of one electron reduction (Table 1).[26] For example, the C_{imine}−N_{imine} distances of 1.321(3) and 1.314(3) Å are elongated from those typically associated with the neutral ligand,[26] while the C_{imine}−C_{ipso} bonds are contracted to 1.435(3) and 1.438(3) Å.

The observation of paramagnetic ground states for both (^{Cy}APDI)CoCl and (^{iPr}APDI)CoCl prompted more detailed studies of the solid state magnetic susceptibility by variable temperature Superconducting Quantum Interference Device (SQUID) magnetometry (Figure 4). Data were collected on three independently prepared, analytically pure samples, and the individual runs were indistinguishable. The data for (^{Cy}APDI)CoCl exhibit a steep decrease in effective magnetic moment as the temperature is lowered, consistent with spin crossover behavior. A maximum of 2.67 μB was observed at 300 K, approaching the spin only value for two unpaired electrons. Accordingly, a solution magnetic moment of 2.5(2) μB was measured in benzene-d_6 at 23 °C. At temperatures below 50 K, the moment drops to 0.23 μB and demonstrates greater population of the singlet state.

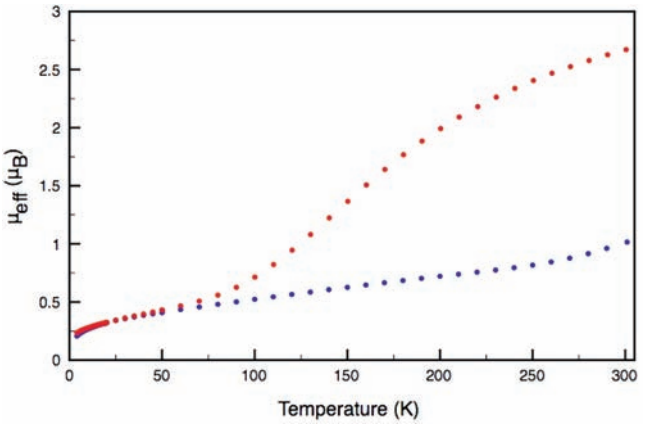

Figure 4. Variable temperature SQUID magnetization data for (^{Cy}APDI)-CoCl (red) and (^{iPr}APDI)CoCl (blue). Data are corrected for underlying diamagnetism.

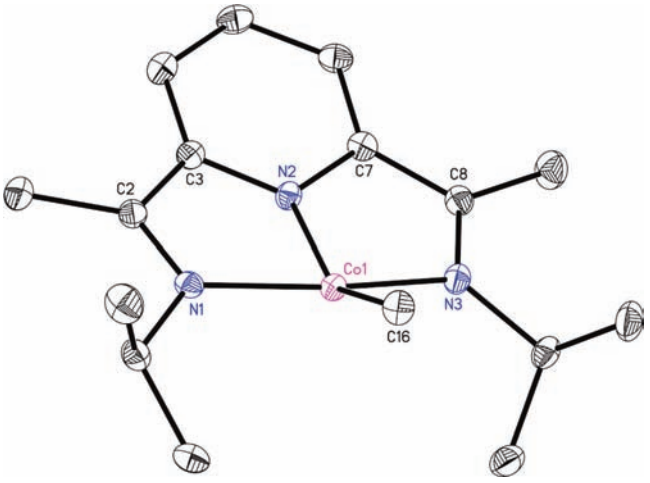

Figure 5. Molecular structure of (^{iPr}APDI)CoMe at 30% probability ellipsoids. Hydrogen atoms omitted for clarity.

The magnetic data for (^{iPr}APDI)CoCl exhibit the same general features as (^{Cy}APDI)CoCl but are overall less pronounced. The effective magnetic moment reaches a maximum of 1.0 μB at 300 K, the highest temperature where data were recorded. The lower maximum magnetic moment for this compound is consistent with the NMR spectroscopic data where a narrower chemical shift dispersion was observed for (^{iPr}APDI)CoCl as compared to (^{Cy}APDI)CoCl. At low temperatures, an effective magnetic moment of 0.21 μB was observed, consistent with population of a singlet state and the value observed for (^{Cy}APDI)CoCl.

The observation of temperature dependent magnetic behavior in both compounds prompted a series of variable temperature ^{1}H NMR experiments. Warming a benzene-d_6 solution of (^{iPr}APDI)CoCl to 65 °C resulted in a broader chemical shift range for the in-plane hydrogen resonances. At this temperature, the chemical shifts of both the imine methyl group (δ = −16.21 ppm) and the *meta*- (δ = 10.83 ppm) and *para*-pyridine (δ = 48.63 ppm) approach the 23 °C values of (^{Cy}APDI)CoCl. Cooling a toluene-d_8 sample of the compound to −60 °C resulted in a contraction of the chemical shift range although the resonances still appeared outside the window typically observed for diamagnetic compounds such

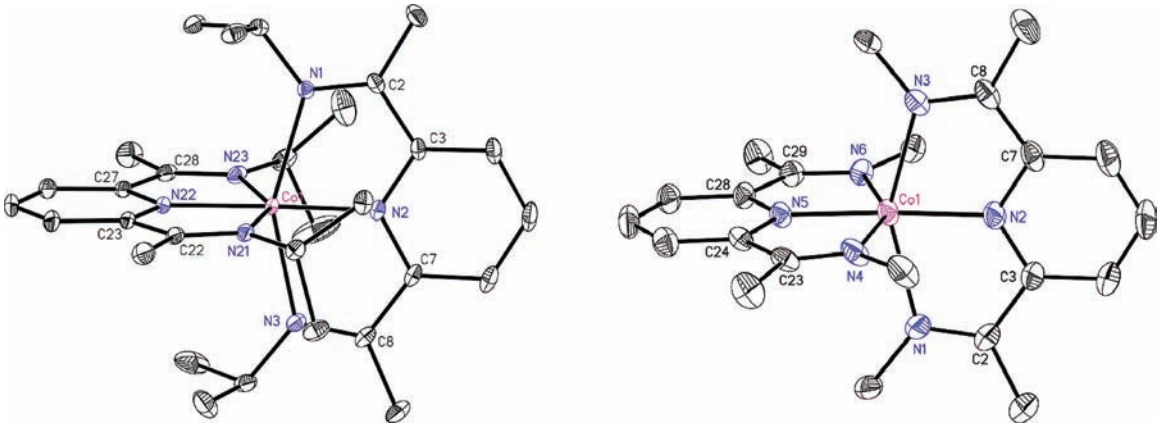

Figure 6. Molecular structures of (^{iPr}APDI)$_2$Co (left) and (^{Cy}APDI)$_2$Co (right) at 30% probability ellipsoids. For (^{Cy}APDI)$_2$Co, the cyclohexyl substituents are omitted for clarity. Hydrogens omitted for clarity in both structures.

as (^{iPr}PDI)CoCl. For example, the imine methyl resonance was observed at −6.24 ppm, while the *meta*- and *para*-pyridine resonances were shifted upfield to 7.81 ppm and 26.10 ppm, respectively.

The spin crossover behavior observed with the (^{R}APDI)-CoCl compounds inspired preparation of the corresponding alkyl derivatives to determine the effect of a stronger field, purely σ-donating ligand on the magnetic behavior and overall electronic structure of the compound. Addition of a slight excess of a 1.6 M diethyl ether solution of MeLi to a toluene solution of either (^{R}APDI)CoCl compound at −95 °C followed by warming to room temperature, filtration, and recrystallization from pentane at −35 °C yielded the desired cobalt methyl complexes, (^{Cy}APDI)CoMe and (^{iPr}APDI)CoMe, as dark red-brown solids in 52 and 81% yields, respectively (eq 2).

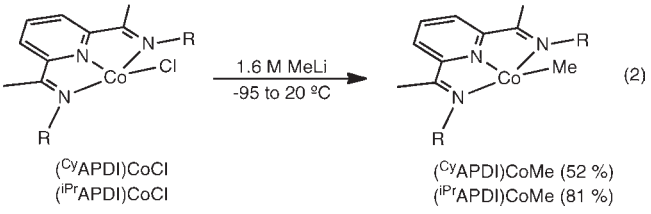

The benzene-d_6 ^{1}H NMR spectra of the (^{R}APDI)CoMe compounds are diagnostic of diamagnetic molecules. Similar to the previously reported *N*-arylated compound, (^{iPr}PDI)-CoMe,[14,19] the in-plane imine methyl groups were observed upfield at 0.13 (R = Cy) and 0.14 (R = ^{i}Pr) ppm, and the *para*-pyridine resonances were located at 9.15 (R = Cy) and 9.41 (R = ^{i}Pr) ppm. Similar chemical shifts were noted by Budzelaar and co-workers in (^{R1}APDI)CoCH$_2$SiMe$_3$ (R^1 = *n*-C$_6$H$_{13}$, *n*-C$_{18}$H$_{37}$) and were accounted for by population of a low-lying triplet excited state.[19]

The solid state structure of (^{iPr}APDI)CoMe was determined by X-ray diffraction, and a representation of the molecule is presented in Figure 5. Selected bond distances and angles are reported in Table 1. As was observed in (^{iPr}APDI)CoCl, the overall geometry of the cobalt methyl complex is best described as distorted square planar with the alkyl group lifted out of the idealized metal-chelate plane. The $N_{pyr}-Co-C_{Me}$ angle of 147.11(8)° is slightly smaller than the value of 150.73(5)° found in the chloro derivative. The $Co-C_{Me}$ bond length of 1.967(2) Å is indistinguishable from the value of 1.960(4) Å reported for (^{iPr}PDI)CoMe.[20] As with (^{iPr}APDI)CoCl, elongated $C_{imine}-N_{imine}$ bonds of 1.326(2) Å and 1.326(2) Å and contracted $C_{imine}-C_{ipso}$ bonds of 1.440(3) Å and 1.434(3) Å were observed, consistent with one electron chelate reduction.[26] It is important to note that the distortions in the solid state structures of (^{iPr}APDI)CoMe and (^{iPr}APDI)-CoCl are similar; however, the electronic structures are different. The alkyl, (^{iPr}APDI)CoMe, is diamagnetic while (^{iPr}APDI)CoCl is paramagnetic at room temperature and exhibits spin crossover behavior. The structural similarity between the two compounds demonstrates that the difference in magnetism and hence electronic structure is not a result of the distortion but rather because of the inherent field strength differences between methyl and chloride.

Two Electron Reduction. Synthesis and Spectroscopy of (^{R}APDI)$_2$Co Compounds. Having established distinct electronic structures for the *N*-arylated and *N*-alkylated one electron reduction products, (^{Ar}PDI)CoCl and (^{R}APDI)-CoCl, the two electron reduction chemistry of (^{R}APDI)CoCl$_2$ was explored. Stirring (^{R}APDI)CoCl$_2$ (R = Cy, ^{i}Pr) with excess 0.5% Na(Hg) under a dinitrogen atmosphere furnished the bis(chelate) cobalt compounds, (^{R}APDI)$_2$Co (R = Cy, ^{i}Pr), in poor (< 40%) yield. With the identity of the product in hand, the synthetic procedure was modified such that an additional equivalent of free bis(imino)pyridine ligand was added to the reduction protocol. This modification as well as performing the reaction under vacuum increased the yield of the bis(chelate) cobalt products to 63% for (^{Cy}APDI)$_2$Co and to 70% for (^{iPr}APDI)$_2$Co (eq 3).

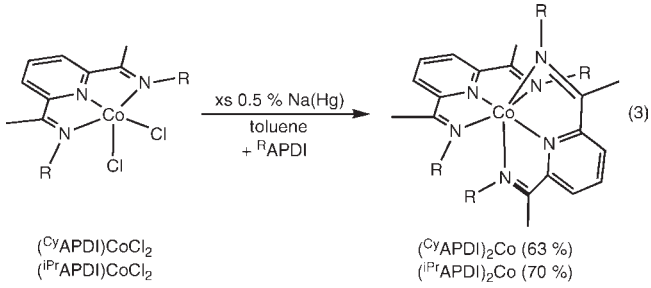

The solid state structures of both compounds were determined by X-ray diffraction and are presented in Figure 6 with selected bond distances and angles reported in Table 2. Also reported in Table 2 are the corresponding

Table 2. Selected Bond Distances (Å) and Angles (deg) for (^{iPr}APDI)$_2$Co, (^{Cy}APDI)$_2$Co, [(^{Cy}APDI)$_2$Co](BF$_4$)$_2$,[8] (^{iPr}APDI)$_2$Fe,[33] and (^{Cy}APDI)$_2$Fe[33] [a]

	(^{iPr}APDI)$_2$Co	(^{Cy}APDI)$_2$Co	[(^{Cy}APDI)$_2$Co](BF$_4$)$_2$	(^{iPr}APDI)$_2$Fe	(^{Cy}APDI)$_2$Fe
M(1)−N(1)	2.2683(9)	2.286(2)	2.221(2)	2.252(2)	2.243(2)
M(1)−N(2)	1.9515(9)	1.9520(19)	2.0079(18)	2.0180(17)	2.005(2)
M(1)−N(3)	2.2408(10)	2.2197(19)	2.273(2)	2.2506(19)	2.221(2)
M(1)−N(4)	2.2484(10)	2.2442(19)	2.219(2)	2.259(2)	2.209(2)
M(1)−N(5)	2.0064(9)	1.9704(18)	2.0084(19)	2.0236(18)	2.005(2)
M(1)−N(6)	2.2236(9)	2.2320(18)	2.250(2)	2.1846(18)	2.277(3)
N(1)−C(2)	1.2985(13)	1.285(3)	1.285(3)	1.316(3)	1.293(4)
N(2)−C(3)	1.3756(14)	1.369(3)	1.341(3)	1.399(3)	1.384(4)
N(2)−C(7)	1.3719(13)	1.381(3)	1.343(3)	1.362(3)	1.375(3)
N(3)−C(8)	1.3029(14)	1.299(3)	1.280(3)	1.299(3)	1.310(3)
C(2)−C(3)	1.4618(16)	1.458(4)	1.496(3)	1.431(3)	1.437(4)
C(7)−C(8)	1.4592(17)	1.451(4)	1.498(3)	1.457(4)	1.442(4)
N(4)−C(23)	1.3175(13)	1.297(3)	1.279(3)	1.312(3)	1.303(3)
N(5)−C(24)	1.3810(16)	1.377(3)	1.339(3)	1.387(3)	1.380(4)
N(5)−C(28)	1.3725(15)	1.384(3)	1.341(3)	1.358(3)	1.386(4)
N(6)−C(29)	1.3044(14)	1.303(3)	1.283(3)	1.304(3)	1.282(4)
C(23)−C(24)	1.4415(17)	1.451(3)	1.492(4)	1.426(3)	1.443(4)
C(28)−C(29)	1.4518(19)	1.450(3)	1.484(4)	1.450(4)	1.445(5)
N(1)−M(1)−N(3)	152.51(3)	152.21(7)	152.56(7)	149.37(7)	149.64(8)
N(4)−M(1)−N(6)	150.41(3)	151.21(7)	152.05(8)	149.06(7)	149.25(9)
N(1)−M(1)−N(4)	93.78(3)	93.70(8)	93.27(8)	94.99(7)	93.01(8)
N(2)−M(1)−N(5)	177.43(4)	177.13(8)	176.24(8)	176.90(8)	176.46(10)

[a] For purposes of the table, the numbering scheme for (^{Cy}APDI)$_2$Co is used for (^{iPr}APDI)$_2$Co and (^{iPr}APDI)$_2$Fe.

distances and angles for the related cobalt dication, [(^{Cy}APDI)$_2$Co](BF$_4$)$_2$,[8] and the neutral iron bis(chelate) compounds, (^{Cy}APDI)$_2$Fe and (^{iPr}APDI)$_2$Fe. For both cobalt compounds, an idealized D_{2d} geometry is observed with essentially orthogonal bis(imino)pyridine chelates. For (^{Cy}APDI)$_2$Co, the N$_{imine}$−Co−N$_{imine}$ angles are 152.21(7)° and 151.74(7)° and the N$_{pyr}$−Co−N$_{pyr}$ angle is 177.13(8)°, while for (^{iPr}APDI)$_2$Co the N$_{imine}$−Co−N$_{imine}$ angles are 152.51(3)° and 151.21(7)° and the N$_{pyr}$−Co−N$_{pyr}$ angle is 177.43(4)°. The deviation of these angles from the ideal 180° is likely caused by the constraints of the bis(imino)pyridine chelate.

Examination of the metrical parameters of (^{Cy}APDI)$_2$Co, presented in Table 2, establishes C$_{imine}$−C$_{ipso}$ bonds lengths that are contracted to ∼1.45 Å compared to the average distance of ∼1.49 Å observed for the neutral ligand bis(chelate) cobalt dication, [(^{Cy}APDI)$_2$Co](BF$_4$)$_2$.[8] The C$_{imine}$−C$_{ipso}$ bonds lengths of (^{iPr}APDI)$_2$Co are also contracted to an average distance of 1.45 Å. The C$_{imine}$−N$_{imine}$ bond lengths for both neutral bis(ligand) complexes are slightly elongated compared to [(^{Cy}APDI)$_2$Co](BF$_4$)$_2$, as would also be expected with ligand reduction.[34] Overall, the C$_{imine}$−C$_{ipso}$ and C$_{imine}$−N$_{imine}$ bond lengths observed for (^{Cy}APDI)$_2$Co and (^{iPr}APDI)$_2$Co are similar to the metrical parameters of the iron analogues, (^{Cy}APDI)$_2$Fe and (^{iPr}APDI)$_2$Fe, which are best described as high-spin iron(II) with two monoreduced bis(imino)pyridine chelates.[33] This indicates that the neutral bis(imino)pyridine cobalt bis(ligand) complexes contain cobalt(II) centers where each chelate is singly reduced.

Both bis(chelate) cobalt complexes are paramagnetic. Effective magnetic moments of 2.6(2) μ_B and 3.0(2) μ_B were measured in benzene-d_6 solution (Evans method[35]) for (^{Cy}APDI)$_2$Co and (^{iPr}APDI)$_2$Co, respectively. One example, (^{iPr}APDI)$_2$Co was studied in the solid state with variable temperature SQUID magnetometry (Figure 7). The effective magnetic moment, μ_{eff}, of (^{iPr}APDI)$_2$Co is nearly temperature independent in the temperature range from 150 to 300 K. The wide plateau at 4.1 μ_B close to the spin-only value of 3.9 μ_B indicates the presence of a well-defined S = 3/2 ground state. Below 150 K the magnetic moment increases unexpectedly to a maximum at 20 K before the values decrease again because of the usual influence of zero-field splitting and magnetization saturation. Since the magnitude of the increase is field dependent and more pronounced at higher field, we infer mechanical torquing, where the small particles of the powder sample are aligned in the magnetic field, as the origin of the unusual behavior.

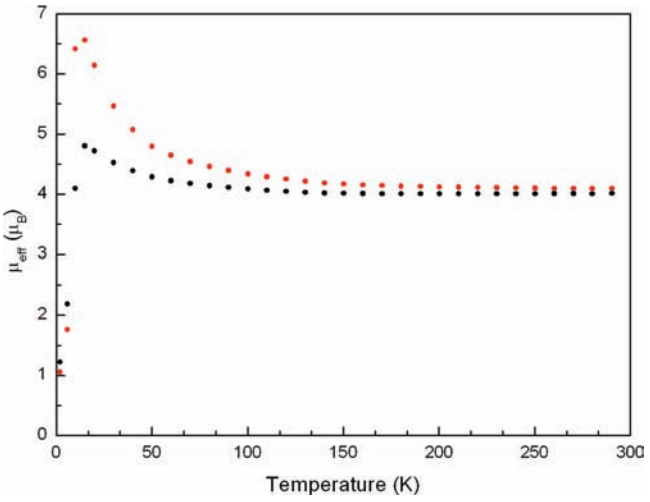

Figure 7. Variable temperature SQUID magnetization data for (^{iPr}APDI)$_2$Co at 1 T (red) and 0.1 T (black).

The electronic structure of the *N*-alkyl substituted cobalt bis(ligand) complexes was also investigated by EPR spectroscopy. The EPR spectrum of (^{iPr}APDI)$_2$Co recorded at 10 K with a powder sample is presented in Figure 8. The spectrum exhibits axial symmetry, with

(34) Bart, S. C.; Chlopek, K.; Bill, E.; Bouwkamp, M. W.; Lobkovsky, E.; Neese, F.; Wieghardt, K.; Chirik, P. J. *J. Am. Chem. Soc.* **2006**, *128*, 13901.
(35) Sur, S. K. *J. Magn. Reson.* **1989**, *82*, 169.

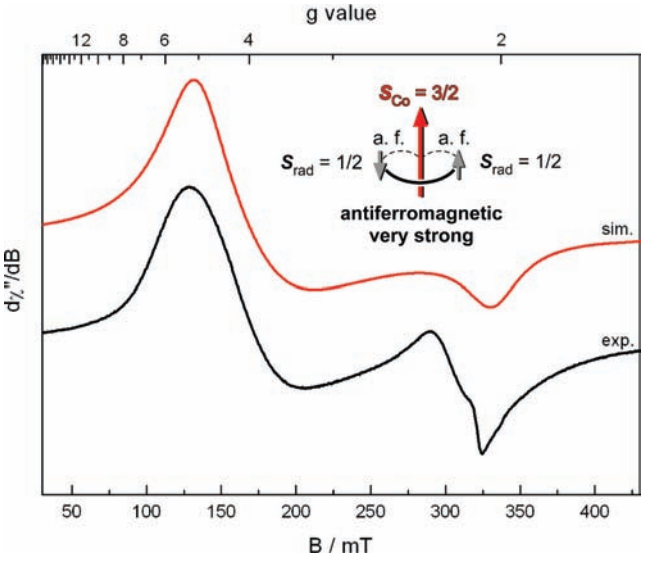

Figure 8. Powder EPR spectrum of (^{iPr}APDI)$_2$Co recorded at 10 K (microwave frequency 9.44 GHz, power 0.63 mW, modulation 2 mT, black trace) and spin Hamiltonian simulation for $S = 3/2$ with $g_{\|} = 2.255$, $g_{\perp} = 2.068$, $E/D \sim 0$, $D = 3$ cm^{-1} and Lorentzian lineshapes (red). The inset visualizes the alignment of Co(II) and ligand spins in the quartet ground state.

effective g values of $g_{\perp}^{eff} = 4.5$ and $g_{\|}^{eff} = 2.1$. The values are typical for a spin quartet, $S = 3/2$, with large axial zero-field splitting ($D \gg h\nu \approx 0.3$ cm^{-1} at X-band) and low rhombicity, $E/D \approx 0$.[36,37] At this condition, the quartet is split by zero-field interaction into two Kramers doublets which can be labeled by magnetic quantum numbers "$m_s = \pm 1/2$" and "$m_s = \pm 3/2$". The "$m_s = \pm 1/2$" doublet has effective g values approximately $g_{\perp}^{eff} = 4$ and $g_{\|}^{eff} = 2$ (for electronic Zeeman g value $g = 2$), whereas the doublet with "$m_s = \pm 3/2$" is virtually EPR silent because of excessive g anisotropy, $g^{eff} \approx (0, 0, 6)$, and vanishing transition probability. Accordingly, the experimental spectrum of (^{iPr}APDI)$_2$Co could be simulated with g values of $g_{\perp} = 2.255$ and $g_{\|} = 2.068$, vanishing rhombicity $E/D \approx 0$, and any value $|D| > 1.0$ cm^{-1};[38] for simplicity the D value was fixed at 3 cm^{-1} (red line, Figure 8). The large line width, which results from intermolecular interactions in the solid, prevents observation of hyperfine coupling. In summary the EPR measurements support the conclusion from magnetic susceptibility that (^{iPr}APDI)$_2$Co has a ground state with total spin of $S = 3/2$.

In comparison to the previously reported corresponding iron complex, (^{iPr}APDI)$_2$Fe, the quartet ground state of (^{iPr}APDI)$_2$Co is counterintuitive. In the iron complex, antiferromagnetic coupling of the two ligand radicals to the high-spin iron(II) center ($S_{Fe} = 2$) dominates radical−radical interaction, which forces the radical spins into a parallel alignment and gives rise to an overall $S = 1$ ground state. One would therefore expect an $S = 1/2$ ground state for the cobalt complex, if the two ligand radicals would also couple antiferromagnetically to the central high-spin Co^{II} ion ($S_{Co} = 3/2$). However, the experimentally observed $S = 3/2$ state indicates that instead antiferromagnetic coupling between the two ligand radicals must dominate over the metal−ligand coupling (Figure 8, inset). This is even more surprising considering the almost perfectly orthogonal arrangement of the two ligand planes (dihedral angle of 88.8°). A more detailed discussion of the electronic ground state of the neutral bis(chelate) complexes will be presented in the computational section.

Synthesis and Spectroscopy of [(^{R}APDI)Co(N$_2$)]$^-$ Compounds. The recent preparation of the aryl-substituted bis(imino)pyridine cobalt dinitrogen anion, [(^{iPr}PDI)CoN$_2$]$^-$, prompted exploration of the synthesis of the corresponding *N*-alkyl substituted compounds.[31] These studies were also designed to explore the feasibility of dinitrogen coordination for an "overreduced" species. Treatment of (^{iPr}APDI)CoCl$_2$ with 3 equiv of sodium naphthalenide, NaC$_{10}$H$_8$, in tetrahydrofuran (THF) under an N$_2$ atmosphere at 23 °C followed by extraction into and recrystallization from Et$_2$O furnished a dark green solid identified as the desired *N*-alkyl substituted bis(imino)pyridine cobalt dinitrogen anion, [Na(solv)$_3$][(^{iPr}APDI)CoN$_2$] (solv = THF, Et$_2$O) as a mixture of THF and Et$_2$O solvates (eq 4). Pure [Na(THF)$_3$][(^{iPr}APDI)CoN$_2$] was obtained by dissolving the isolated material in THF followed by solvent removal.

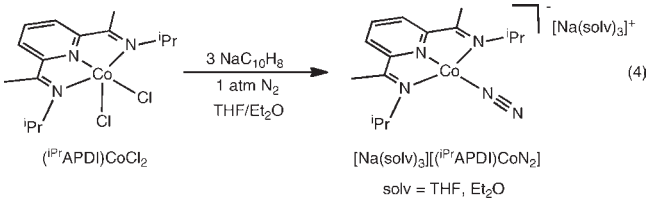

The *N*-alkyl substituted bis(imino)pyridine cobalt dinitrogen anions were characterized by infrared and NMR spectroscopies. The THF solvate, [Na(THF)$_3$][(^{iPr}APDI)CoN$_2$], exhibited a strong N≡N stretch at 1991 cm^{-1} in the KBr infrared spectrum. This value is at lower frequency than the corresponding diethyl etherate value of 2037 cm^{-1}. The difference in N$_2$ stretching frequencies for the different solvates is likely a result of the different coordination mode or degree of interaction of the sodium counterion with the chelate or dinitrogen ligand. Similar effects have been noted by Gambarotta in various modified *N*-aryl substituted bis(imino)pyridine iron dinitrogen anions,[39] as well as with the analogous *N*-aryl substituted complexes [Na(solv)$_3$][(^{iPr}PDI)CoN$_2$].[31]

The ^{1}H NMR spectrum of [Na(THF)$_3$][(^{iPr}APDI)CoN$_2$] was recorded in a 1:1 mixture of benzene-d_6 and THF to dissolve the ion pair, and the chemical shifts are indicative of a pure diamagnetic molecule without contamination from thermally accessible triplet excited states (as in (^{Ar}PDI)CoX and (^{R}APDI)Co-alkyl compounds). For example, the singlet for the in-plane imine methyl resonance appears at 2.24 ppm while the *para*-pyridine hydrogen was located at 6.68 ppm.

One electron oxidation of [Na(THF)$_3$][(^{iPr}APDI)CoN$_2$] in the presence of 1 atm of N$_2$ was explored with the goal of synthesizing the elusive neutral, four-coordinate cobalt dinitrogen complex. Unfortunately, addition of 1 equiv of [Cp$_2$Fe][BPh$_4$] to a diethyl ether solution of [Na(solv)$_3$][(^{iPr}APDI)CoN$_2$] furnished a brown solid identified as the

(36) Banci, L.; Bencini, A.; Benelli, C.; Gatteschi, D.; Zanchini, C. In *Structure and Bonding*; Springer Verlag: Berlin/Heidelberg, 1982; Vol. *52*, p 36.
(37) Benelli, C.; Gatteschi, D. *Inorg. Chem.* **1982**, *21*, 1788.
(38) Bencini, A.; Benelli, C.; Gatteschi, D.; Zanchini, C. *Inorg. Chem.* **1979**, *18*, 2137.
(39) Scott, J.; Vidyaratne, I.; Korobkov, I.; Gambarotta, S.; Budzelaar, P. H. M. *Inorg. Chem.* **2008**, *47*, 896.

Table 3. Comparison of Computed and Experimental Bond Distances (Å) and Angles (deg) for (^{iPr}APDI)CoX (X = Cl, Me) Compounds

	(^{iPr}APDI)CoCl		(^{iPr}APDI)CoMe	
	exp.	calc.	exp.	calc.
Co(1)−N(1)	1.9334(15)	2.003	1.9103(16)	1.985
Co(1)−N(2)	1.7870(16)	1.838	1.8072(16)	1.869
Co(1)−N(3)	1.9203(16)	2.003	1.9228(16)	1.983
Co(1)−Cl	2.2188(6)	2.249	1.967(2)	1.990
N(1)−C(2)	1.321(3)	1.318	1.326(2)	1.326
N(2)−C(3)	1.371(2)	1.372	1.373(2)	1.369
N(2)−C(7)	1.371(2)	1.372	1.383(2)	1.369
N(3)−C(8)	1.314(3)	1.318	1.326(2)	1.326
C(2)−C(3)	1.435(3)	1.453	1.440(3)	1.452
C(7)−C(8)	1.438(3)	1.453	1.434(3)	1.452
N(2)−Co(1)−X	150.73(5)	156.34	147.11(8)	147.66
	(^{iPr}PDI)CoCl		(^{iPr}PDI)CoMe	
	exp.	calc.	exp.	calc.
Co(1)−N(1)	1.916(3)	1.978	1.907(3)	1.973
Co(1)−N(2)	1.797(3)	1.833	1.834(3)	1.879
Co(1)−N(3)	1.912(3)	1.978	1.903(3)	1.971
Co(1)−Cl	2.1807(10)	2.212	1.960(4)	1.973
N(1)−C(2)	1.322(5)	1.320	1.335(4)	1.329
N(2)−C(3)	1.373(5)	1.372	1.366(4)	1.367
N(2)−C(7)	1.369(6)	1.372	1.365(4)	1.367
N(3)−C(8)	1.317(5)	1.320	1.329(4)	1.328
C(2)−C(3)	1.444(5)	1.451	1.443(5)	1.450
C(7)−C(8)	1.435(5)	1.451	1.434(6)	1.449
N(2)−Co(1)−X	179.15	179.85	178.93	179.28

bis(chelate) cobalt compound, (^{iPr}APDI)$_2$Co, with no evidence for any other cobalt species (eq 5). It is interesting that the *N*-alkylated bis(imino)pyridine ligand will support an anionic cobalt dinitrogen complex but not a neutral one.

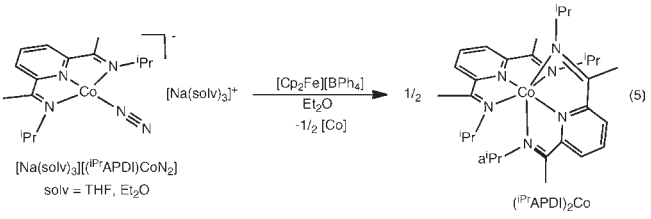

Computational Studies. The electronic structures of the *N*-alkyl substituted bis(imino)pyridine cobalt halide, alkyl, and bis(chelate) compounds were examined by density functional theory (DFT). Previous work from our laboratories has demonstrated the utility of the combination of DFT, spectroscopy, and magnetochemistry for identifying chelate participation in the electronic structure of reduced bis(imino)pyridine iron[26b,33] and cobalt[31] compounds. Several questions guided these studies:

(i) What is the origin of the deviation from square planar geometry observed for (^{R}APDI)CoCl and (^{R}APDI)CoMe compounds that is absent in the corresponding *N*-aryl substituted ^{Ar}PDI compounds?

(ii) What is the origin of the observed spin crossover behavior in (^{R}APDI)CoCl and why are these compounds different from (^{R}APDI)CoMe, although the same structural distortion is observed in the solid state structure?

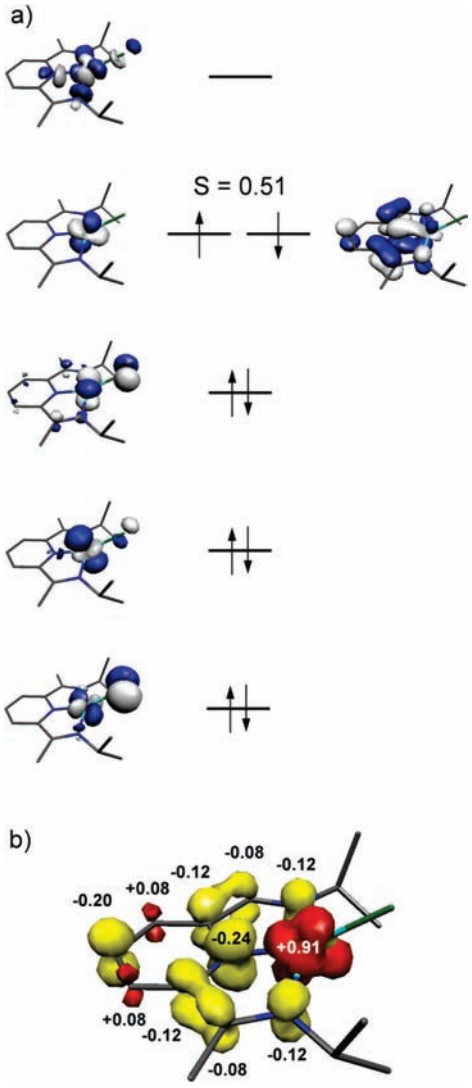

Figure 9. (a) Qualitative molecular orbital diagram for the $S = 0$ state (^{iPr}APDI)CoCl computed from a broken symmetry BS(1,1) B3LYP DFT calculation. (b) Spin density plot obtained from a Mulliken population analysis (red, positive spin density; yellow, negative spin density). The coordinate system is defined as "z" perpendicular to the idealized plane of the ^{iPr}APDI ligand and "x" along the N_{pyr}−Co vector.

(iii) What are the electronic structures of the (^{R}APDI)$_2$Co derivatives and how do they compare to related iron compounds?[33]

Previous DFT studies by Budzelaar and co-workers established an open-shell singlet ground state for (^{Ar}PDI)CoX and (^{R}APDI)CoX (X = H, Me, Cl) arising from antiferromagnetic coupling of a low spin Co^{II} ion ($S_{Co} = 1/2$) with a bis(imino)pyridine radical anion ($S_{PDI} = 1/2$).[19] All complexes were predicted to be square planar independent of the imine substituents, which is in contradiction to the experimental data provided for (^{R}APDI)CoX (X = Me, Cl; R = ^{i}Pr, Cy) in this work. Nonplanar structures were only found for hydride and methyl complexes optimized at the restricted DFT level. These restricted solutions, however, were computed to be 10−20 kcal/mol less stable than the planar structures obtained from the unrestricted calculations.

Broken symmetry (BS) DFT calculations were performed at the B3LYP level to understand the electronic structures of (^{R}APDI)CoMe and (^{R}APDI)CoCl and to

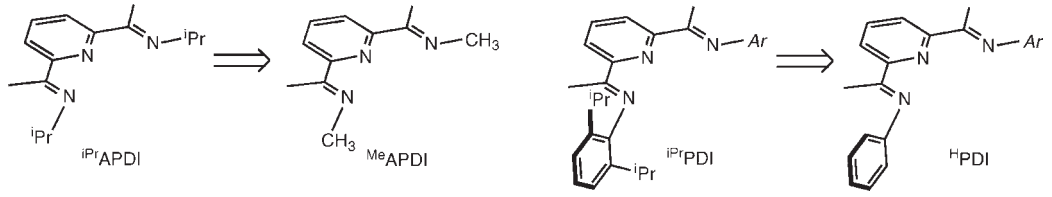

Figure 10. Truncated versions of the bis(imino)pyridine ligands used for DFT studies to examine the origin of the observed distortion in (^{R}APDI)CoCl compounds.

compare the geometric preferences to the corresponding *N*-arylated ^{R}PDI analogues (Table 3). Both (^{iPr}APDI)CoX and (^{iPr}PDI)CoX (X = Me, Cl) were chosen as representative examples of the two classes of compounds and have also been crystallographically characterized. In each case, the molecules were computed without truncations. In agreement with the experimentally determined diamagnetic, low-temperature ground states, the geometries were optimized using a BS(1,1) approach corresponding to a low spin Co^{II} ion antiferromagnetically coupled to a bis(imino)pyridine radical anion. A qualitative molecular orbital (MO) diagram derived from these results for (^{iPr}APDI)CoCl is shown in Figure 9 and illustrates the common open-shell singlet ground state of all four complexes at low temperature. In conformity with the results reported by Budzelaar,[19] the closed-shell ground states, for example, ($APDI^{0}$)Co^{I}Cl, for all complexes obtained via the restricted DFT method were found to be significantly higher in energy.

To investigate the steric effects of the imine substituents on the N_{pyr}−Co−X angle, truncated versions of the chloride complexes were investigated in silico (Figure 10). For this purpose, the isopropyl groups on the aryl substituents of ^{iPr}PDI were replaced by hydrogen atoms (^{H}PDI), and the isopropyl substituents of ^{iPr}APDI were replaced by methyl groups (^{Me}APDI). For both complexes, (^{H}PDI)CoCl and (^{Me}APDI)CoCl, square planar structures were obtained after geometry optimization independent of the initial N_{pyr}−Co−X angle (180° or 150°). In a second experiment, the methyl groups on the imine backbone of ^{iPr}APDI were replaced by hydrogen atoms. Again, a planar structure was obtained after optimization of the corresponding Co−Cl complex. This indicates that the distortion from planarity observed for diamagnetic (^{iPr}APDI)CoCl and (^{Cy}APDI)-CoCl at low temperatures is a result of the steric influence of the bulky secondary alkyl substituents on the imines in combination with the methyl group of the ligand backbone and is not due to electronic effects.

Finally, the origin of the spin-crossover phenomenon experimentally observed for (^{iPr}APDI)CoCl was investigated by DFT. It has been shown that modern hybrid DFT functionals are slightly biased towards high spin solutions because of the admixture of exact Hartree−Fock exchange. It is therefore challenging to predict the correct ground state multiplicities for transition metal complexes. Nevertheless, it has been suggested that small, predicted energy differences in favor of the high spin state may be considered indicative of spin-crossover behavior.[40]

To separate electronic from steric effects, calculations were first carried out on the sterically truncated model complex, (^{Me}APDI)CoCl. A simple unrestricted DFT approach assuming a triplet state resulted in an electronic structure as described by Budzelaar and co-workers.[19] The Co^{II} ion possesses a low spin d^7 configuration with one unpaired electron located in the d_{z^2} orbital, while the second unpaired electron occupies a bis(imino)pyridine π symmetry orbital. In agreement with the previous calculations,[19] this state lies 3.1 kcal/mol above the open-shell singlet and retains preference for the square planar geometry of the BS(1,1) state. A different triplet state was obtained from a BS(3,1) calculation. In this solution, the ligand π radical is antiferromagnetically coupled to a high spin Co^{II} center (d^7, S_{Co} = 3/2). Surprisingly, this electronic configuration was found to

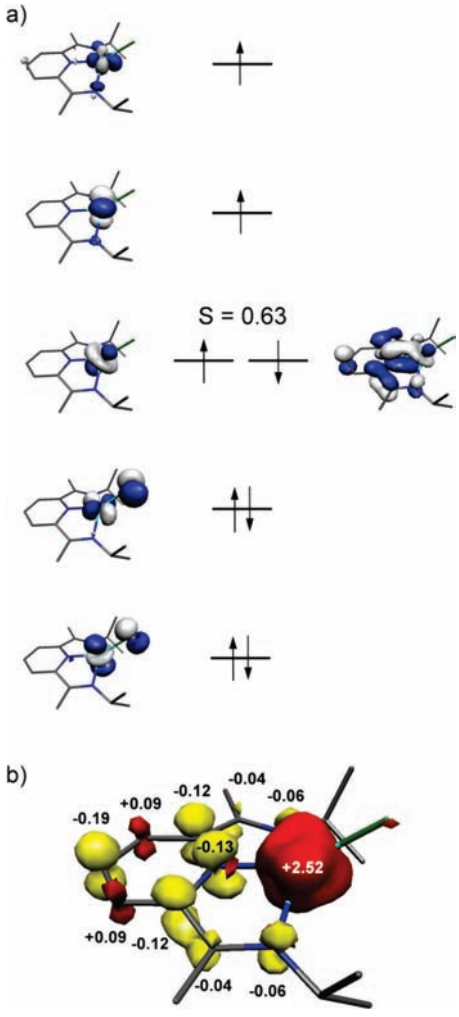

Figure 11. (a) Qualitative molecular orbital diagram for the S = 1 state of (^{iPr}APDI)CoCl computed from a broken symmetry BS(3,1) B3LYP DFT calculation. (b) Spin density plot obtained from a Mulliken population analysis (red: positive spin density, yellow: negative spin density). The coordinate system is defined as "z" perpendicular to the idealized plane of the ^{iPr}APDI ligand and "x" along the N_{pyr}−Co vector.

(40) Ye, S.; Neese, F. *Inorg. Chem.* **2010**, *49*, 772.

Table 4. Comparison of Computed and Experimental Bond Distances (Å) and Angles (deg) for (^{iPr}APDI)$_2$Co

	(^{iPr}APDI)$_2$Co	
	exp.	calc.
Co(1)−N(1)	2.2683(9)	2.270
Co(1)−N(2)	1.9515(9)	1.992
Co(1)−N(3)	2.2408(10)	2.238
Co(1)−N(4)	2.2236(9)	2.242
Co(1)−N(5)	2.0064(9)	1.992
Co(1)−N(6)	2.2484(10)	2.262
N(1)−C(2)	1.2985(13)	1.320
N(2)−C(3)	1.3756(14)	1.383
N(2)−C(7)	1.3719(13)	1.384
N(3)−C(8)	1.3029(14)	1.322
C(2)−C(3)	1.4618(16)	1.467
C(7)−C(8)	1.4592(17)	1.464
N(4)−C(23)	1.3044(14)	1.322
N(5)−C(24)	1.3725(15)	1.384
N(5)−C(28)	1.3810(16)	1.383
N(6)−C(29)	1.3175(13)	1.321
C(23)−C(24)	1.4518(19)	1.465
C(28)−C(29)	1.4415(17)	1.466
N(1)−Co(1)−N(3)	152.51(3)	151.86
N(4)−Co(1)−N(6)	150.41(3)	151.88
N(1)−Co(1)−N(4)	91.13(4)	93.60
N(2)−Co(1)−N(5)	177.43(4)	178.91

be only 0.1 kcal/mol less stable than the open-shell singlet solution obtained from the BS(1,1) calculation with a low spin Co^{II} ion and thus is more stable than the simple unrestricted triplet. More importantly, the optimized structure for the BS(3,1) triplet is significantly bent with a N$_{pyr}$−Co−Cl angle of 153.55°. Because of the absence of bulky substituents in (^{Me}APDI)CoCl this distortion must be exclusively due to electronic effects.

For (^{iPr}APDI)CoCl, the BS(3,1) state is found to be 6.6 kcal/mol more stable than the BS(1,1) open-shell singlet state. This is clearly due to a destabilization of the singlet state by the bulky isopropyl groups enforcing a bent structure and promoting the spin-crossover behavior. In the bent molecule, the d_{yz} orbital is destabilized by strong π donation of the Cl ligand, while the $d_{x^2-y^2}$ orbital is stabilized, so that the energy gap between these two orbitals decreases and favors a high spin Co^{II} center. A qualitative MO diagram for the $S = 1$ state of (^{iPr}APDI)CoCl is presented in Figure 11. Accordingly, the corresponding complex (^{iPr}APDI)CoMe containing a purely σ donating methyl ligand exhibits no spin-crossover behavior because of the absence of the destabilization of the d_{yz} orbital. In fact, all attempts to calculate a BS(3,1) solution for this complex converged back to the unrestricted triplet solution in spite of the sterically enforced lifting of the Me ligand.

For the *N*-aryl substituted PDI complexes, similar computational results were obtained. For the sterically less demanding complex, (^{H}PDI)CoCl, a small BS(1,1) singlet−BS(3,1) triplet gap of 4.7 kcal/mol was calculated in favor of the triplet state. In addition, the structure shows a lifting of the Cl ligand with a N$_{pyr}$−Co−Cl angle of 141.20°. However, the introduction of the bulky 2,6-isopropyl substituents in (^{iPr}PDI)CoCl forces the molecule into a more planar geometry in the triplet state (N$_{pyr}$−Co−Cl angle of 159.93°) and decreases the singlet−triplet gap to 0.5 kcal/mol. These computational results imply that the experimentally observed spin-crossover phenomena in *N*-alkyl

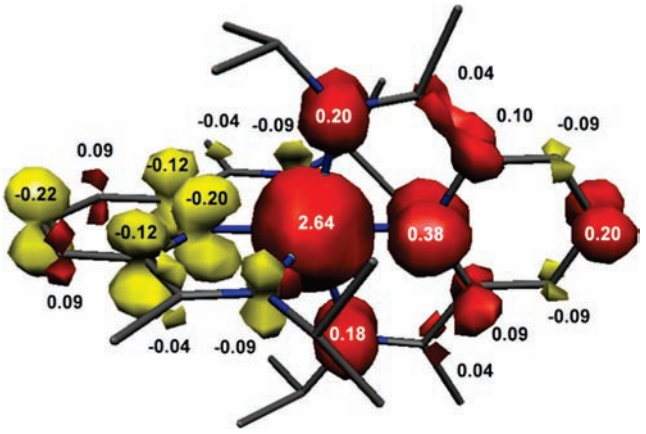

Figure 12. Spin density plot for (^{iPr}APDI)$_2$Co derived from a Mulliken spin population analysis of the BS(4,1) calculation (red, positive spin density; yellow, negative spin density).

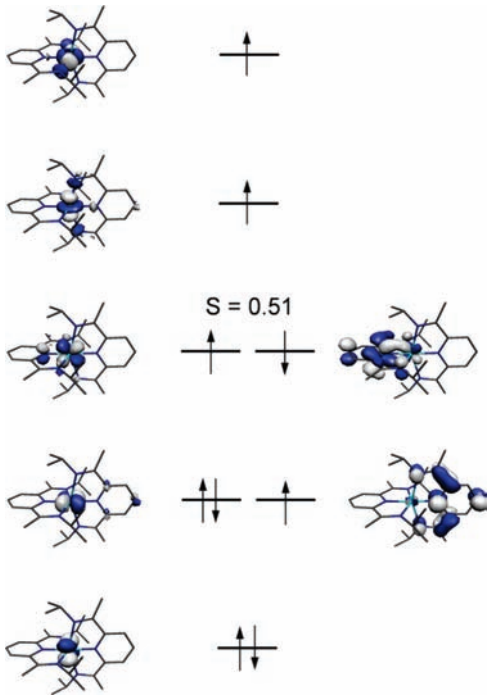

Figure 13. Qualitative molecular orbital diagram for (^{iPr}APDI)$_2$Co from a B3LYP DFT calculation. The coordinate system is defined as "*z*" perpendicular to the idealized plane of the ^{iPr}APDI ligand and "*y*" along the N$_{pyr}$−Co vector.

substituted (^{Cy}APDI)CoCl and (^{iPr}APDI)CoCl are due to a high spin/low spin transition of the central Co^{II} ion (S_{Co} = 3/2 → 1/2) associated with a lifting of the Cl ligand out of the idealized metal-chelate plane. The energy gap between the BS(1,1) singlet and the BS(3,1) triplet state is modified by the steric influence of the imine substituents.

The electronic structure of the bis(chelate) cobalt complex, (^{iPr}APDI)$_2$Co, was also investigated by DFT calculations. The ground state geometry was optimized using the experimentally determined $S = 3/2$ ground state with the BP86 functional. The experimental and calculated geometric structures are in excellent agreement (Table 4).

Single point calculations on the optimized structure were performed at the B3LYP level of DFT. The simple unrestricted approach assuming a quartet ground state

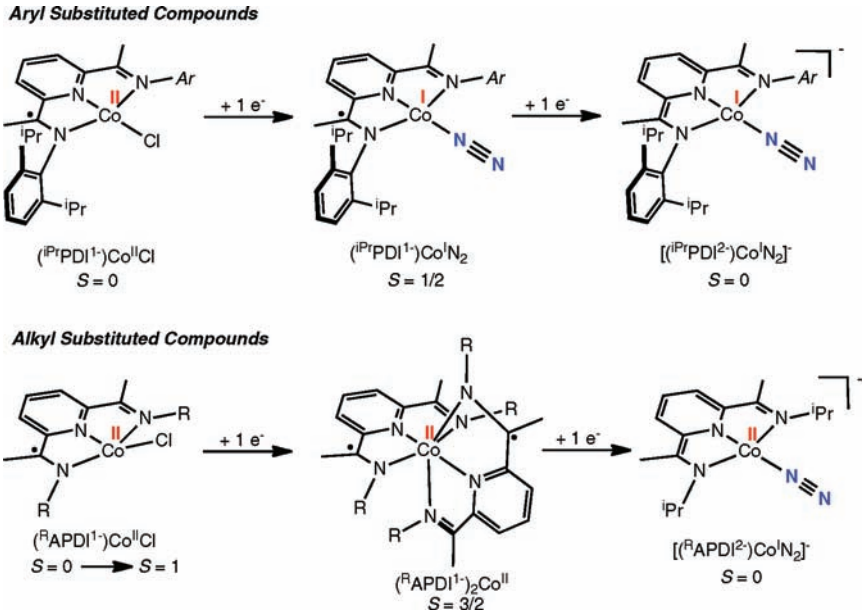

Figure 14. Electronic structure summary and comparison of reduced *N*-aryl versus *N*-alkyl substituted bis(imino)pyridine cobalt complexes.

resulted in spontaneous symmetry breaking to a BS(4,1) solution. The obtained electronic structure is consistent with a high-spin Co^{II} ion ($S_{Co} = 3/2$) and two ligand-centered radicals. This is similar to the situation encountered for the corresponding iron complex (^{iPr}APDI)$_2$Fe, which contains a high spin ferrous ion (d^6, $S_{Fe} = 2$) and two ligand radicals, one on each bis(imino)pyridine ligand.[33] In the iron complex, the two ligand π radical singly occupied molecular orbitals (SOMOs) are antiferromagnetically coupled to two degenerate t_{2g} orbitals (d_{xy} and d_{yz}) of the metal ion resulting in a parallel alignment of the ligand spins and a total spin of $S = 1$. In the cobalt complex, in contrast, the two ligand radical spins are aligned in an antiparallel fashion. This can most clearly be deduced from the spin density plot shown in Figure 12 where the sum of the spin densities on each ligand is close to one, but of opposite sign.

The corresponding qualitative MO diagram obtained from the calculation is shown in Figure 13. Compared to the analogous iron complex, the high spin Co^{II} ion (d^7) possesses one more electron in the t_{2g} set, which leaves one t_{2g} SOMO (d_{yz}) available for antiferromagnetic coupling to a ligand radical, while the d_{xy} orbital is filled. The remaining metal SOMOs (d_{z^2} and $d_{x^2-y^2}$) comprise the e_g set and are orthogonal to the π radical SOMO of the second ligand resulting in ferromagnetic coupling. This description of the electronic structure of (^{iPr}APDI)$_2$Co is, however, a gross oversimplification of the true ground state and is due to the failure of the BS wave function to accurately describe the multireference character of such radical systems. Because of the symmetry of the complex, a second degenerate solution exists, in which the spin densities on the ligands are inverted and one of the unpaired electrons resides in the d_{xy} orbital, while the d_{yz} orbital is doubly occupied. Consequently, the ground state of the molecule is the superposition of both states where the ligand radicals are antiferromagnetically coupled to each other and form a diamagnetic pair that carries no spin density. The antiferromagnetic coupling between the two orthogonal ligand π systems is mediated through a doubly occupied MO of the degenerate d_{yz} and d_{xy} set via a superexchange pathway reminiscent of the radical−radical coupling in square-planar, singlet-diradical Ni complexes described by Neese and co-workers.[41] This coupling must be stronger than the antiferromagnetic coupling between the Co center and the two radicals, which is due to the half-filled orbital of the $d_{yz}-d_{xy}$ set (Figure 8). The spin density of three unpaired electrons is completely localized on the Co center.

A summary and comparison of the electronic structures of both the *N*-aryl and *N*-alkyl substituted bis(imino)-pyridine cobalt complexes is presented in Figure 14. One salient difference is with the formally one electron (from the corresponding (PDI)$CoCl_2$) reduced monochloride compounds where the *N*-alkyl substituted derivatives access triplet ground states at higher temperatures while the corresponding *N*-alkyl compounds are diamagnetic over all temperatures reported. The two electron reduced products, again using (PDI)$CoCl_2$ as the starting point, differ both structurally and electronically. For the *N*-arylated cases, the sterically demanding chelates support neutral dinitrogen complexes where the reduction occurs at the cobalt. In the *N*-alkyl compounds, bis(chelate) formation is observed and the cobalt(II) oxidation state is maintained and the second reduction event is ligand based.

Conclusions

Replacing the *N*-aryl substituents on the bis(imino)pyridine chelates with alkyl groups has a profound impact on the molecular and electronic structures of reduced cobalt halide, alkyl, and bis(ligand) complexes. Whereas (^{Ar}PDI$^-$)$Co^{II}Cl$ compounds are diamagnetic over all temperatures examined and are essentially planar, the alkylated variants, (^{iPr}APDI$^-$)-$Co^{II}Cl$ and (^{Cy}APDI$^-$)$Co^{II}Cl$ are spin crossover compounds with distorted geometries where the chloride ligand is lifted out of the idealized metal-chelate plane. Computational

(41) Herebian, D.; Wieghardt, K.; Neese, F. *J. Am. Chem. Soc.* **2003**, *125*, 10997.

studies suggest that the deviation from planarity is steric rather than electronic in origin. The spin crossover behavior is related to the non-planarity of the molecule and arises from spin state changes at the Co(II), d^7 ion. At low temperature, the low-spin $S_{Co} = 1/2$ configuration antiferromagnetically couples to ($^{R}APDI^{-}$) giving rise to an overall diamagnetic molecule. As the temperature is increased, contributions from high spin Co(II), $S_{Co} = 3/2$ increase, and antiferromagnetic coupling with the ligand centered radical yields a triplet state. Note in both forms, a singly reduced bis(imino)pyridine chelate antiferromagnetically coupled to at least one cobalt-based unpaired electron is constant.

Two electron reduction of ($^{R}APDI^{0}$)$Co^{II}Cl_2$ furnished the bis(chelate) cobalt complexes, ($^{R}APDI^{-}$)$_2Co^{II}$. Spectroscopic, magnetic and computational data establish quartet ground states arising from a high spin Co(II), d^7 ion ($S_{Co} = 3/2$) and two singly reduced bis(imino)pyridine radical anions. In this description, the two ligand-centered radical spins are antiparallel and antiferromagnetically coupled to each other by mediation of filled, degenerate d_{yz} and d_{xy} cobalt orbitals. This electronic structure is distinct from the related bis(chelate) iron complexes, ($^{R}APDI^{-}$)$_2Fe^{II}$, where a triplet ground state is observed arising from a high spin iron center ($S_{Fe} = 2$) antiferromagnetically coupled to two chelate radical anions. The difference in electronic structures is a result of the additional electron in a t_{2g}-type orbital in the cobalt case that *diminishes* antiferromagnetic coupling between the metal and the chelate electrons but *promotes* coupling between the ligand radicals. Thus, ligand participation in the overall electronic structure of the metal complex is a synergistic interaction influenced by the specific d electron configuration and orbital occupancy.

Experimental Section

General Considerations. All air- and moisture-sensitive manipulations were carried out using standard vacuum line, Schlenk, and cannula techniques or in an MBraun inert atmosphere drybox containing an atmosphere of purified nitrogen. Solvents for air- and moisture-sensitive manipulations were initially dried and deoxygenated using literature procedures.[42] Benzene-d_6 was purchased from Cambridge Isotope Laboratories and dried over 4 Å molecular sieves.

^{1}H NMR spectra were recorded on Varian Mercury 300, Inova 400, 500, and 600 spectrometers operating at 299.76, 399.78, 500.62, and 599.78 MHz, respectively. ^{13}C NMR spectra were recorded on an Inova 500 spectrometer operating at 125.893 MHz. All ^{1}H and ^{13}C NMR chemical shifts are reported relative to $SiMe_4$ using the ^{1}H (residual) and ^{13}C chemical shifts of the solvent as a secondary standard. Peak widths at half heights are reported for paramagnetically broadened and shifted resonances. Solution magnetic moments were determined by Evans method[35] using a ferrocene standard and are the average value of at least two independent measurements. Gouy balance measurements were performed with a Johnson Matthey instrument that was calibrated with $HgCo(SCN)_4$. Peak widths at half heights are reported for paramagnetically broadened and shifted resonances. Infrared spectra were collected on a Thermo Nicolet spectrometer. Elemental analyses were performed at Robertson Microlit Laboratories, Inc., in Madison, NJ.

Single crystals suitable for X-ray diffraction were coated with polyisobutylene oil in a drybox, transferred to a nylon loop, and then quickly transferred to the goniometer head of a Bruker X8 APEX2 diffractometer equipped with a molybdenum X-ray tube ($\lambda = 0.71073$ Å). Preliminary data revealed the crystal system. A hemisphere routine was used for data collection and determination of lattice constants. The space group was identified and the data were processed using the Bruker SAINT+ program and corrected for absorption using SADABS. The structures were solved using direct methods (SHELXS) completed by subsequent Fourier synthesis and refined by full-matrix least-squares procedures.

SQUID magnetization data of crystalline powdered samples were recorded with a SQUID magnetometer (Quantum Design) at 10 kOe between 5 and 300 K for all samples. Values of the magnetic susceptibility were corrected for the underlying diamagnetic increment by using tabulated Pascal constants and the effect of the blank sample holders. Samples used for magnetization measurement were recrystallized multiple times and checked for chemical composition by ^{1}H NMR spectroscopy. The program julX written by E. Bill was used for (elements of) the simulation and analysis of magnetic susceptibility data.[43]

Quantum-Chemical Calculations. All DFT calculations were performed with the ORCA program package.[44] The geometry optimizations of the complexes and single-point calculations on the optimized geometries were carried out at the B3LYP level[45−47] of DFT. This hybrid functional often gives better results for transition metal compounds than pure gradient-corrected functionals, especially with regard to metal−ligand covalency.[48] The all-electron Gaussian basis sets were those developed by the Ahlrichs group.[49,50] Triple-ζ quality basis sets TZVP with one set of polarization functions on the metals and on the atoms directly coordinated to the metal center were used.[50] For the carbon and hydrogen atoms, slightly smaller polarized split-valence SV(P) basis sets were used, that were of double-ζ quality in the valence region and contained a polarizing set of d-functions on the non-hydrogen atoms.[49] Auxiliary basis sets used to expand the electron density in the resolution-of-the-identity (RI) approach were chosen,[51−53] to match the orbital basis.

The SCF calculations were tightly converged (1×10^{-8} E_h in energy, 1×10^{-7} E_h in the density change, and 1×10^{-7} in maximum element of the DIIS error vector). The geometry optimizations for all complexes were carried out in redundant internal coordinates without imposing symmetry constraints. In all cases the geometries were considered converged after the energy change was less than 5×10^{-6} E_h, the gradient norm and maximum gradient element were smaller than 1×10^{-4} E_h Bohr^{-1} and 3×10^{-4} E_h Bohr^{-1}, respectively, and the root-mean square and maximum displacements of all atoms were smaller than 2×10^{-3} Bohr and 4×10^{-3} Bohr, respectively.

Throughout this paper we describe our computational results by using the broken-symmetry (BS) approach by Ginsberg[54] and Noodleman.[55] Because several broken symmetry solutions to the spin-unrestricted Kohn−Sham equations may be obtained,

(42) Pangborn, A. B.; Giardello, M. A.; Grubbs, R. H.; Rosen, R. K.; Timmers, F. J. *Organometallics* **1996**, *15*, 1518.

(43) http://ewww.mpi-muelheim.mpg.de/bac/logins/bill/julX_en.php.

(44) Neese, F. *Orca - an ab initio, DFT and Semiempirical Electronic Structure Package*, Version 2.7, Revision 0; Institut für Physikalische und Theoretische Chemie, Universität Bonn: Bonn, Germany, August 2009.

(45) Becke, A. D. *J. Chem. Phys.* **1986**, *84*, 4524.

(46) Becke, A. D. *J. Chem. Phys.* **1993**, *98*, 5648.

(47) Lee, C. T.; Yang, W. T.; Parr, R. G. *Phys. Rev. B* **1988**, *37*, 785.

(48) Neese, F.; Solomon, E. I. In *Magnetism: From Molecules to Materials*; Miller, J. S., Drillon, M., Eds.; Wiley: New York, 2002; Vol. *4*, p 345.

(49) Schäfer, A.; Horn, H.; Ahlrichs, R. *J. Chem. Phys.* **1992**, *97*, 2571.

(50) Schäfer, A.; Huber, C.; Ahlrichs, R. *J. Chem. Phys.* **1994**, *100*, 5829.

(51) Eichkorn, K.; Weigend, F.; Treutler, O.; Ahlrichs, R. *Theor. Chem. Acc.* **1997**, *97*, 119.

(52) Eichkorn, K.; Treutler, O.; Öhm, H.; Häser, M.; Ahlrichs, R. *Chem. Phys. Lett.* **1995**, *240*, 283.

(53) Eichkorn, K.; Treutler, O.; Öhm, H.; Häser, M.; Ahlrichs, R. *Chem. Phys. Lett.* **1995**, *242*, 652.

(54) Ginsberg, A. P. *J. Am. Chem. Soc.* **1980**, *102*, 111.

(55) Noodleman, L.; Peng, C. Y.; Case, D. A.; Mouesca, J. M. *Coord. Chem. Rev.* **1995**, *144*, 199.

the general notation BS(m,n)[56,16] has been adopted, where m (n) denotes the number of spin-up (spin-down) electrons at the two interacting fragments.

Canonical and corresponding[57] orbitals, as well as spin density plots were generated with the program Molekel.[58]

Preparation of 2,6-(^{i}PrN=CMe)$_2$C$_5$H$_3$N (^{iPr}APDI). This compound was synthesized by a modification of the literature procedure.[59] A 250 mL round-bottom flask was charged with 3.00 g (18.38 mmol) of 2,6-diacetylpyridine, approximately 100 mL of isopropyl amine, and a magnetic stir bar. *p*-Toluenesulfonic acid (0.340 g, 1.97 mmol) was added, and the reaction was heated to a reflux for 3 days. The solution was cooled to ambient temperature, and excess isopropyl amine was removed in vacuo. The resulting tan solid was extracted into dichloromethane, washed with 2 × 100 mL water and 100 mL saturated sodium bicarbonate solution, and dried over $MgSO_4$. The solution was filtered, the volatiles were removed in vacuo, and the resulting solid was recrystallized from methanol at −35 °C to yield 1.30 g (28%) of off-white plates identified as ^{iPr}APDI.[59]

Preparation of (^{Cy}APDI)CoCl$_2$. This compound was synthesized by a modification of the literature procedure.[8] A 100 mL round-bottom flask was charged with 0.507 g (1.56 mmol) of ^{Cy}APDI and 0.184 g (1.42 mmol) of $CoCl_2$. Approximately 50 mL of THF were added to the flask, and the resulting mixture was stirred for 12 h during which time a pale green precipitate formed. The solid was collected by filtration and washed with pentane to yield 0.627 g (94%) of a pale green powder identified as (^{Cy}APDI)CoCl$_2$. ^{1}H NMR (CD_2Cl_2): δ = −59.37 (170.8 Hz, 4H, Cy CH_2), −35.44 (237.9 Hz, 4H, Cy CH_2), −21.44 (133.6 Hz, 6H, C(CH_3)), −18.79 (149.8 Hz, 4H, Cy CH_2), −9.64 (123.3 Hz, 4H, Cy CH_2), −7.64 (121.3 Hz, 2H, Cy CH_2), −4.93 (17.7 Hz, 1H, *p-pyridine*), −3.38 (150.7 Hz, 2H, Cy CH_2), 77.92 (162.2 Hz, 2H, *m-pyridine* or Cy C*H*), 84.91 (151.1 Hz, 2H, *m-pyridine* or Cy C*H*).

Preparation of (^{iPr}APDI)CoCl$_2$. This compound was prepared in a similar manner to (^{Cy}APDI)CoCl$_2$ with 0.489 g (1.99 mmol) of ^{iPr}APDI and 0.246 g (1.89 mmol) of $CoCl_2$ yielding 0.717 g (96%) of a gray-green solid identified as (^{iPr}APDI)CoCl$_2$. Analysis for $C_{15}H_{23}N_3CoCl_2$: Calcd C, 48.02; H, 6.18; N, 11.20. Found C, 47.94; H, 5.85; N, 10.94. Magnetic susceptibility (Gouy balance, 293 K): μ_{eff} = 4.2(2) μ_B. ^{1}H NMR (CD_2Cl_2): δ = −38.23 (111.0 Hz, 12H, CH(CH_3)$_2$), −20.26 (60.5 Hz, 6H, C(CH_3)), −2.30 (58.2 Hz, 1H, *p-pyridine*), 74.39 (4.6 Hz, 2H, *m-pyridine* or C*H*(CH$_3$)$_2$), 87.14 (4.6 Hz, 2H, *m-pyridine* or C*H*(CH$_3$)$_2$).

Preparation of (^{Cy}APDI)CoCl. A 100 mL round-bottom flask was charged with 0.171 g (0.376 mmol) of ^{Cy}APDICoCl$_2$, approximately 50 mL of toluene and a stir bar. The toluene slurry was cooled in a liquid nitrogen chilled cold well, $NaEt_3BH$ (376 μL of a 1.0 M solution in toluene, 0.376 mmol) was added dropwise with stirring. The reaction was warmed to ambient temperature with stirring. Upon warming a gradual color change to bright purple occurred, and the resulting purple solution was filtered through Celite and concentrated. The solution was cooled to −35 °C and yielded 0.099 g (63%) of a dark red-brown solid identified as (^{Cy}APDI)CoCl. Analysis for $C_{21}H_{31}N_3Co$: Calcd C, 60.07; H, 7.44; N, 10.01. Found C, 59.87; H, 7.64; N, 9.80. Magnetic susceptibility (benzene-d_6, 296 K): μ_{eff} = 2.5(2) μ_B. ^{1}H NMR (benzene-d_6): δ = −22.79 (57.6 Hz, 6H, C(CH_3)), −4.38 (48.5 Hz, 4H, Cy CH_2), 0.55 (50.0 Hz, 4H, Cy CH_2), 0.65 (63.5 Hz, 4H, Cy CH_2), 1.50 (67.1 Hz, 6H, Cy CH_2), 2.47 (56.7 Hz, 2H, Cy CH_2), 8.72 (45.9 Hz, 2H, Cy C*H*), 12.07 (41.8 Hz, 2H, *m-pyridine*), 66.27 (76.5 Hz, 1H, *p-pyridine*).

Preparation of (^{iPr}APDI)CoCl. This compound was prepared in a similar manner to (^{Cy}PDI)CoCl with 0.544 g (1.45 mmol) of (^{iPr}APDI)CoCl$_2$ and $NaEt_3BH$ (1450 μL of a 1.0 M solution in toluene, 1.45 mmol). The resulting dark mauve solid was recrystallized from diethyl ether at −35 °C yielding 0.294 g (60%) of dark mauve crystals identified as (^{iPr}APDI)CoCl. Analysis for $C_{15}H_{23}N_3CoCl$: Calcd C, 53.03; H, 6.82; N, 12.37. Found C, 53.17; H, 6.79; N, 12.24. Magnetic susceptibility (benzene-d_6, 296 K): μ_{eff} = 1.0(2) μ_B. ^{1}H NMR (benzene-d_6): δ = −12.62 (47.4 Hz, 6H, C(CH_3)), 0.42 (47.1 Hz, 12H, CH(CH_3)$_2$), 7.20 (51.8 Hz, 2H, C*H*(CH$_3$)$_2$), 9.52 (42.1 Hz, 2H, *m-pyridine*), 41.6 (71.6 Hz, 1H, *p-pyridine*).

Preparation of (^{Cy}APDI)CoMe. A 20 mL scintillation vial was charged with 0.204 g (0.486 mmol) of (^{Cy}APDI)CoCl, approximately 15 mL of toluene, and a magnetic stir bar. The solution was frozen in a liquid nitrogen cooled cold well, and MeLi (425 μL of a 1.6 M solution in diethyl ether, 0.680 mmol) was added to the thawing solution. The reaction mixture was warmed to ambient temperature with stirring and then filtered through Celite. The volatiles were removed in vacuo, and the resulting dark purple solid was recrystallized from diethyl ether at −35 °C to yield 0.100 g (52%) of a dark red-brown solid identified as (^{Cy}APDI)CoMe. Analysis for $C_{22}H_{34}N_3Co$: Calcd C, 66.15; H, 8.58; N, 10.52. Found C, 66.04; H, 8.24; N, 10.04. ^{1}H NMR (benzene-d_6): δ = 0.13 (s, 6H, C(CH_3)), 1.41 (m, 2H, Cy C$^4H_2$), 1.56 (m, 4H, Cy C$^3H_2$), 1.70 (m, 2H, Cy C$^4H_2$), 1.78 (m, 4H, Cy C$^3H_2$), 2.36 (m, 4H, Cy C$^2H_2$), 2.53 (m, 4H, Cy C$^2H_2$), 3.37 (s, 3H, Co−CH_3), 4.65 (m, 2H, Cy C^1H), 7.35 (d, 7.6 Hz, 2H, *m-pyridine*), 9.41 (t, 7.6 Hz, 1H, *p-pyridine*). ^{13}C {^{1}H} NMR (benzene-d_6): δ = 21.16 (C(*C*H$_3$)), 26.42 (Cy *C*^{3}H$_2$), 26.70 (Cy *C*^{4}H$_2$), 32.11 (Cy *C*^{2}H$_2$), 70.77 (Cy *C*^{1}H), 111.09 (*p-pyridine*), 126.61 (*m-pyridine*), 146.63 (*o-pyridine*), 158.87 (*C*(CH$_3$)), one resonance not located.

Preparation of (^{iPr}APDI)CoMe. This compound was prepared using a similar method to (^{Cy}APDI)CoMe using 0.136 g (0.400 mmol) (^{iPr}APDI)CoCl and MeLi (350 μL of a 1.6 M solution in diethyl ether, 0.560 mmol). Recrystallization from diethyl ether at −35 °C yielded 0.104 g (81%) of a dark red solid identified as (^{iPr}APDI)CoMe. Analysis for $C_{16}H_{26}N_3Co$: Calcd C, 60.18; H, 8.21; N, 13.16. Found C, 60.04; H, 8.18; N, 13.18. ^{1}H NMR (benzene-d_6): δ = 0.14 (s, 6H, C(CH_3)), 1.78 (d, 6.6 Hz, 12H, CH(CH_3)$_2$, 2.05 (s, 3H, Co−CH_3), 5.01 (septet, 6.6 Hz, 2H, C*H*(CH$_3$)$_2$), 7.30 (d, 7.6 Hz, 2H, *m-pyridine*), 9.15 (t, 7.6 Hz, 1H, *p-pyridine*). ^{13}C {^{1}H} NMR (benzene-d_6): δ = 20.49 (C(*C*H$_3$)), 22.06 (CH(*C*H$_3$)$_2$), 60.78 (*C*H(CH$_3$)$_2$), 112.49 (*p-pyridine*), 123.74 (*m-pyridine*), 147.68 (*o-pyridine*), 158.43 (*C*(CH$_3$)), one resonance not located.

Preparation of (^{iPr}APDI)$_2$Co. A thick walled glass vessel was charged with 28.2 g of Hg (140.6 mmol) and approximately 100 mL of toluene. Sodium metal (0.141 g, 6.13 mmol) was added in small pieces, and the resulting amalgam was stirred for 15 min. The flask was cooled in a cold well at liquid nitrogen temperature followed by addition of (^{iPr}APDI)CoCl$_2$ (0.460 g, 1.23 mmol) and ^{iPr}APDI (0.301 g, 1.23 mmol). The flask was fitted with a 180° needle valve and quickly removed from the drybox and submerged in liquid nitrogen. The solution was degassed four times on a high vacuum line, and the reaction was warmed to room temperature and stirred for 16 h, during which time a color change to red was observed. The solution was filtered through Celite, the volatiles were removed in vacuo, and the remaining red-brown solid was recrystallized from pentane at −35 °C to yield 0.108 g (70%) of red crystals identified as (^{iPr}APDI)$_2$Co. Analysis for $C_{30}H_{46}N_6Co$: Calcd C, 65.55; H, 8.43; N, 15.29. Found C, 65.28; H, 8.46; N, 15.22. Magnetic susceptibility (293 K): μ_{eff} = 3.6(2) μ_B. ^{1}H NMR (benzene-d_6): δ = −64.35 (193.3 Hz, 2H, *p-pyridine*), −4.32 (77.4 Hz, 24H, CH(CH_3)$_2$), 46.24 (119.0 Hz, 4H, *m-pyridine* or C*H*(CH$_3$)$_2$),

(56) Kirchner, B.; Wennmohs, F.; Ye, S.; Neese, F. *Curr. Opin. Chem. Biol.* **2007**, *11*, 134.
(57) Neese, F. *J. Phys. Chem. Solids* **2004**, *65*, 781.
(58) *Molekel, Advanced Interactive 3D-Graphics for Molecular Sciences*; Swiss National Supercomputing Centre: Manno, Switzerland; available under http://www.cscs.ch/molkel/.
(59) Castro, P. M.; Lappalainen, K.; Ahlgrén, M.; Leskelä, M.; Repo, T. *J. Polym. Sci., Part A: Polym, Chem.* **2003**, *41*, 1380–1389.

64.49 (189.0 Hz, 12H, C(CH_3)), 185.13 (211.0 Hz, 4H, *m-pyridine* or C*H*(CH_3)$_2$).

Preparation of (^{Cy}APDI)$_2$Co. This compound was prepared in a similar manner to (^{iPr}APDI)$_2$Co with 25.0 g (124.6 mmol) of Hg, 0.125 g (5.44 mmol) of sodium metal, 0.355 g (1.09 mmol) of ^{Cy}APDI, and 0.496 g (1.09 mmol) of (^{Cy}APDI)CoCl$_2$. Recrystallization of the resulting red-brown solid from pentane at −35 °C yielded 0.485 g (63%) of dark red-brown crystals identified as (^{Cy}APDI)$_2$Co. Analysis for $C_{42}H_{62}N_6Co$: Calcd C, 71.06; H, 8.80; N, 11.84. Found C, 70.71; H, 8.42; N, 11.45. Magnetic susceptibility (293 K): μ_{eff} = 3.0(2) μ_B. ^{1}H NMR (benzene-d_6): δ = −62.361 (938.1 Hz, 2H, *p-pyridine*), −21.11 (83.2 Hz, 8H, Cy CH_2), −8.67 (197.2 Hz, 8H, Cy CH_2), −3.53 (31.2 Hz, 8H, Cy CH_2), 0.26 (20.8 Hz, 4H, Cy CH_2), 2.34 (7.1 Hz, 4H, Cy CH_2), 6.51 (30.7 Hz, 8H, Cy CH_2), 47.91 (140.0 Hz, 4H, *m-pyridine* or Cy C*H*), 61.09 (30.9 Hz, 12H, C(CH_3)), 178.17 (9.1 Hz, 4H, *m-pyridine* or Cy C*H*).

Preparation of [Na(solv)$_3$][(^{iPr}APDI)Co(N$_2$)] (solv = THF, Et$_2$O). Sodium naphthalenide was prepared in situ by addition of approximately 50 mL of THF to a 100 mL round-bottom flask containing 0.072 g (3.13 mmol) of sodium metal and 0.402 g (3.13 mmol) of naphthalene. The reaction was stirred for 3 h during which time a green solution formed and the solids had dissolved. Small portions totaling 0.335 g (0.893 mmol) of (^{iPr}APDI)CoCl$_2$ were added to the flask, and the reaction was stirred for 1 h after which time the volatiles were removed. The residual solid was extracted into diethyl ether and stirred for 1 h to give a bright green solution. The solution was filtered through Celite, concentrated and cooled to −35 °C to yield 0.366 g (71%) of dark green crystals identified as a mixture of [Na(Et$_2$O)$_3$][(^{iPr}APDI)Co(N$_2$)] along with [Na(THF)$_3$][(^{iPr}APDI)Co(N$_2$)]. Dissolution of the dark green crystals in THF followed by removal of volatiles gave quantitative yield of a dark green powder identified as [Na(THF)$_3$][(^{iPr}APDI)Co(N$_2$)]. ^{1}H NMR (1:1 THF-d_8/benzene-d_6): δ = 1.89 (s, 12H, CH(CH_3)$_2$), 2.24 (s, 6H, C(CH_3)), 4.70 (s, 2H, C*H*(CH_3)$_2$), 6.68 (s, 1H, *p-pyridine*), 8.04 (s, 2H, *m-pyridine*). IR (KBr): ν_{NN} = 2037 cm^{-1} (solv = Et$_2$O), 1991 cm^{-1} (solv = THF).

Oxidation of [Na(Et$_2$O)$_3$][(^{iPr}APDI)Co(N$_2$)] with [Cp$_2$Fe][BPh$_4$]. A 20 mL scintillation vial was charged with 0.036 g (0.062 mmol) of [Na(Et$_2$O)$_3$][(^{iPr}APDI)Co(N$_2$)], approximately 5 mL of diethyl ether, and a stir bar, yielding a bright green solution. 0.031 g (0.061 mmol) of Cp$_2$Fe was added by spatula, and the reaction was stirred for 1 h. A color change to brown was observed. The solution was filtered though Celite, and volatiles were removed to give a dark brown solid. Formation of (^{iPr}APDI)$_2$Co and Cp$_2$Fe was confirmed by ^{1}H NMR spectroscopy.

Acknowledgment. We thank the U.S. National Science Foundation and the Deutsche Forschungsgemeinschaft for a Cooperative Activities in Chemistry between U.S. and German Investigators grant.

Supporting Information Available: Crystallographic details for (^{iPr}APDI)CoCl, (^{iPr}APDI)CoCMe, (^{iPr}APDI)$_2$Co, and (^{Cy}APDI)$_2$Co in cif format. This material is available free of charge via the Internet at http://pubs.acs.org.